

STOCHASTIC MODELING AND REGULARITY OF THE NONLINEAR ELLIPTIC CURL–CURL EQUATION

ULRICH RÖMER^{†§}, SEBASTIAN SCHÖPS^{†‡¶}, AND THOMAS WEILAND[†]

Abstract. This paper addresses the nonlinear elliptic curl–curl equation with uncertainties in the material law. It is frequently employed in the numerical evaluation of magnetostatic fields, where the uncertainty is ascribed to the so-called B – H curve. A truncated Karhunen–Loève approximation of the stochastic B – H curve is presented and analyzed with regard to monotonicity constraints. A stochastic nonlinear curl–curl formulation is introduced and numerically approximated by a finite element and collocation method in the deterministic and stochastic variable, respectively. The stochastic regularity is analyzed by a higher order sensitivity analysis. It is shown that, unlike to linear and several nonlinear elliptic problems, the solution is not analytic with respect to the random variables and an algebraic decay of the stochastic error is obtained. Numerical results for both the Karhunen–Loève expansion and the stochastic curl–curl equation are given for illustration.

Key words. nonlinear, uncertainties, Karhunen–Loève, regularity, stochastic collocation

AMS subject classifications. 78A30, 65N15, 65N35, 65N30, 65N12

1. Introduction. Today, it is increasingly acknowledged that uncertainty quantification is an important part within simulation based design. It allows to control the risk of failure as technical devices are designed and operated closer to their physical limits. When the underlying physics are modelled by partial differential equations, uncertain inputs are typically identified with the material’s constitutive relation, geometries, initial data or boundary values. In particular the case of random material coefficients for linear equations has received considerable attention in recent years, see [26, 52, 9, 6] among others. In electromagnetics the coefficients are frequently modeled to be piecewise constant on subdomains. In a stochastic setting, which is adapted here, neglecting anisotropy, on each subdomain the material coefficient can be represented by a single random variable. An important exception is the magnetic properties of ferromagnetic materials, that, in the anhysteretic case, are expressed through a map

$$(1.1) \quad |\mathbf{H}(\mathbf{x})| = f(|\mathbf{B}(\mathbf{x})|),$$

where \mathbf{H} and \mathbf{B} are the magnetic field and flux density, respectively. Magnetic saturation effects, incorporated through the nonlinear dependency on the field magnitude, cannot be neglected in many situations and have been found to be sensitive to uncertainties. In this setting the input randomness is modelled by an infinite-dimensional random field and its discretization must be accomplished. This is complicated by the fact, that each trajectory of the material law has to fulfill smoothness and shape requirements. An example of a material law is given in Figure 1 on the left, showing

[†]Technische Universitaet Darmstadt, Institut für Theorie Elektromagnetischer Felder, Schloßgartenstrasse 8, D–64289 Darmstadt

[‡]Technische Universitaet Darmstadt, Graduate School of Computational Engineering, Dolivostraße 15, D–64293 Darmstadt

[§]Supported by the ”Deutsche Forschungsgemeinschaft” (DFG) under SFB 634

[¶]Supported by the ”Excellence Initiative” of the German Federal and State Governments and the Graduate School of Computational Engineering at Technische Universitaet Darmstadt, the FP7-ICT-2013-11 Project nanoCOPS: Nanoelectronic COupled Problems Solutions and the ”Bundesministerium für Bildung und Forschung” (BMBF) SIMUROM project.

clearly a monotonic behavior of f . An important aspect of this work is the shape-aware modelling of uncertainties in view of a constraint for the derivative

$$(1.2) \quad 0 < \alpha \leq \frac{\partial f(\cdot, s)}{\partial s} \leq \beta < \infty, \quad s \geq 0.$$

To this end, in the literature, closed-form parametric material models have been employed. Among others, we mention different forms of the Brillouin model, see, e.g., [48, 45] or the Brauer model [12]. These models are appealing due to their simplicity and a physical interpretation of the parameters can often be given. Finite dimensional random fields are readily obtained by using random- instead of deterministic parameters. However, there is a lack of flexibility due to the a priori fixed dimensionality and specific shape of the analytical functions used. Moreover, the model parameters have been found to be correlated [45] and the model might not be used directly in stochastic simulations. The (linear) truncated Karhunen–Loève expansion [35, 29] is known to be a flexible and efficient tool to approximate random fields with high accuracy and to separate stochastic and deterministic variables. It is applied in this paper in view of a stochastic material law with regularity and shape constraints (1.2). The regularity can be controlled by the smoothness of the covariance function whereas the shape constraints imply restrictions on the truncation order, or alternatively, on the uncertainty magnitude. It is observed that this magnitude is dependent on the correlation length of the process, in accordance with [8, pp. 1281–1283] in the context of uniform coercivity constraints. Numerical examples with data supported from measurements given in [45] support the findings.

Given random material input data, we discuss a stochastic nonlinear magneto-static formulation. For related work see [48, 12] and [18] for the full set of (linear) Maxwell’s equations in a stochastic setting. Following a frequently used procedure in the literature [8, 39], we first analyze the modelling error arising in magnetic fields through the truncation of the Karhunen–Loève expansion. Then the problem is reformulated as a high dimensional deterministic one and an approximation scheme is presented. The scheme involves linearization, as well as a finite element and collocation approximation in the deterministic and stochastic variable, respectively. We analyze the stochastic regularity to establish the convergence rate of the numerical procedure. A complication arises here due to the specific type of the nonlinearity. In particular the implicit function theorem cannot be applied and no analytic dependency of the solution with respect to the random variables is obtained. Instead, finite differentiability is established using the chain rule and the deterministic regularity of the solution. Numerical examples will complement the findings. Let us also mention, that the problem considered here is related to many other physical problems, e.g., nonlinear heat conduction. In two dimensions the equations reduce to a nonlinear version of the Poisson equation.

The paper is structured as follows. After a brief description of the magnetostatic model problem in Section 2, we introduce randomness in the material law, present the truncated Karhunen–Loève expansion and analyze the respective truncation error in the stochastic problem in Section 3. In Section 4 we will outline the stochastic collocation method and establish its convergence. This involves a higher order sensitivity analysis w.r.t. the stochastic variables. Finally, in Section 5 convergence results will be illustrated by numerical examples.

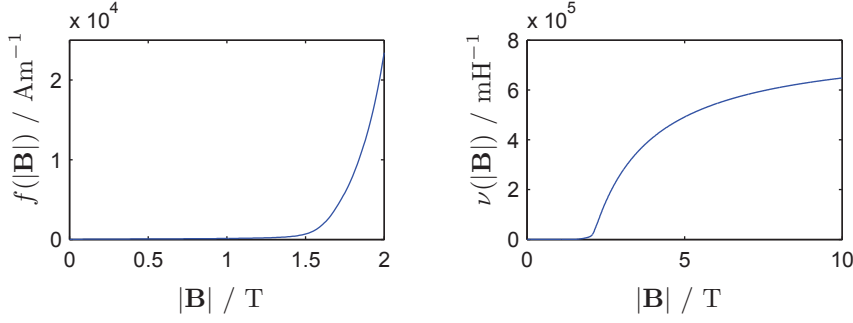


FIG. 1. *Left: example of a nonlinear magnetic material law based on real data. Right: associated magnetic reluctivity, satisfying $\lim_{x \rightarrow \infty} \nu(x) = \nu_0$.*

1.1. Notation. Boldface type is used for vectors $\mathbf{u} = (u_1, u_2, u_3)$ and vector-functions. Important function spaces are

$$(1.3) \quad V := \mathcal{H}_0(\mathbf{curl}; D) = \{\mathbf{u} \in L^2(D)^3 \mid \mathbf{curl} \mathbf{u} \in L^2(D)^3 \text{ and } \mathbf{u} \times \mathbf{n} = 0, \text{ on } \partial D\},$$

and for $s > 0$

$$(1.4) \quad \mathcal{H}^s(\mathbf{curl}, D) := \{\mathbf{u} \in \mathcal{H}^s(D)^3 \mid \mathbf{curl} \mathbf{u} \in \mathcal{H}^s(D)^3\},$$

see [37]. We write $(\cdot, \cdot)_2$ for the $L^2(D)^3$ -inner product and $\|\cdot\|_2$ for the associated norm.

The Euclidean norm is denoted by $|\cdot|$. Also, we introduce the notation $g^{(i)} := \partial_x^i g(x)$ for the i -th derivative of a function. For $I \subset \mathbb{R}^n$, open and bounded, $\mathcal{C}^k(\bar{I})$ denotes the space of k -times differentiable functions with bounded and uniformly continuous derivatives up to order k , endowed with the norm

$$(1.5) \quad \|g\|_{\mathcal{C}^k(\bar{I})} := \max_{0 \leq i \leq k} \sup_{x \in I} |g^{(i)}(x)|.$$

The sets of real non-negative and positive numbers are denoted \mathbb{R}_0^+ and \mathbb{R}^+ , whereas \mathbb{N}_0, \mathbb{N} refer to the sets of natural numbers with and without zero, respectively.

We also need a multi-index notation: for $\gamma \in \mathbb{N}_0^M$, let $\partial_{\mathbf{y}}^{\gamma} := \frac{\partial^{|\gamma|_1}}{\partial y_1^{\gamma_1} \dots \partial y_M^{\gamma_M}}$, for $|\gamma|_1 := \sum_i \gamma_i > 0$ and $\partial_{\mathbf{y}}^0$ be the identity operator. For two multi-indices, $\gamma_1 < \gamma_2$ holds true if $\gamma_1 \leq \gamma_2$ holds true component-wise and if $\gamma_1 \neq \gamma_2$. Also, to a multi-index γ with $|\gamma|_1 = n$, we associate a set γ with n entries, such that $\partial^n / \prod_{i \in \gamma} \partial_{y_i} = \partial_{\mathbf{y}}^{\gamma}$ see [38, p.518].

2. The Model Problem. We consider the magnetostatic problem on a domain D ,

$$(2.1a) \quad \mathbf{curl} \mathbf{H} = \mathbf{J}, \quad \text{in } D,$$

$$(2.1b) \quad \text{div} \mathbf{B} = 0, \quad \text{in } D,$$

$$(2.1c) \quad \mathbf{B} \cdot \mathbf{n} = 0, \quad \text{on } \partial D,$$

with outer unit normal \mathbf{n} and divergence free electric current density $\text{div} \mathbf{J} = 0$. We introduce the magnetic vector potential \mathbf{A} , such that $\mathbf{curl} \mathbf{A} = \mathbf{B}$. Then using the

material law (1.1), equations (2.1) are transformed into a second order **curl-curl** problem

$$\begin{aligned} (2.2a) \quad & \mathbf{curl}(\nu(|\mathbf{curl} \mathbf{A}|) \mathbf{curl} \mathbf{A}) = \mathbf{J}, & \text{in } D, \\ (2.2b) \quad & \mathbf{A} \times \mathbf{n} = 0, & \text{on } \partial D, \end{aligned}$$

supplemented with the Coulomb gauge

$$(2.2c) \quad \operatorname{div} \mathbf{A} = 0, \quad \text{in } D.$$

In (2.2a), ν refers to the magnetic reluctivity, defined by

$$(2.3) \quad \nu(\cdot, s) := \frac{f(\cdot, s)}{s}, \quad s > 0.$$

Although ν is the coefficient appearing in the differential equations measurement results are typically given directly for f and thus both will be included in the discussion. Note that, in contrast to f , ν is not necessarily monotonic. From now on we simplify the situation and neglect the spatial dependency in f , i.e., $f(\mathbf{x}, \cdot) = f(\cdot)$, by abuse of notation. An adaption to the important case of piecewise constant material properties is achieved by minor modifications, see also Remark 1. In absence of hysteresis and anisotropy, the nonlinear magnetic material law can be described, following [47, 44], by a bijective function

$$(2.4) \quad f : \mathbb{R}_0^+ \rightarrow \mathbb{R}_0^+ : |\mathbf{B}| \mapsto |\mathbf{H}| = f(|\mathbf{B}|).$$

Following [44], properties of the deterministic material law f are summarized in the following assumption.

ASSUMPTION 1. *It holds for the deterministic material law that*

$$\begin{aligned} (2.5a) \quad & f \text{ is continuously differentiable,} \\ (2.5b) \quad & 0 < \alpha \leq f^{(1)}(s) \leq \beta < \infty, \\ (2.5c) \quad & f(0) = 0, \\ (2.5d) \quad & \lim_{s \rightarrow \infty} f^{(1)}(s) = \beta. \end{aligned}$$

As f might have increased differentiability properties, we refer to (2.5a) as minimal regularity assumption. Note, that β can be identified with the reluctivity of vacuum ν_0 . Depending on the problem formulation it might be more convenient to work with the inverse law f^{-1} . However, in this case similar assumptions can be made.

LEMMA 2.1. *Let Assumption 1 be satisfied, then the magnetic reluctivity satisfies for all $s \in \mathbb{R}_0^+$*

$$\begin{aligned} (2.6a) \quad & \nu \text{ is continuous and } \alpha \leq \nu(s) \leq \beta, \\ (2.6b) \quad & s \mapsto \nu(s)s \text{ is strongly monotone,} \\ (2.6c) \quad & s \mapsto \nu(s)s \text{ is Lipschitz continuous,} \end{aligned}$$

with monotonicity and Lipschitz constants α, β , respectively.

Proof. See, e.g., [43]. \square

2.1. The Nonlinear curl-curl Formulation. We proceed with the derivation of a weak formulation of the model problem and a result on existence and uniqueness of a solution. Throughout the paper, we consider a bounded, simply connected polyhedral Lipschitz domain D . A weak formulation of (2.2) relies on

$$(2.7) \quad \hat{V} = \{\mathbf{u} \in V \mid (\mathbf{u}, \mathbf{grad} \varphi)_2 = 0, \quad \forall \varphi \in \mathcal{H}_0^1(D)\},$$

the space of functions in V with weak zero divergence. We recall from [32, Corollary 4.4] that the Poincaré–Friedrichs–type inequality

$$(2.8) \quad \|\mathbf{u}\|_2 \leq C_F \|\mathbf{curl} \mathbf{u}\|_2$$

holds, for all $\mathbf{u} \in \hat{V}$ and \hat{V} can be endowed with the norm $\|\mathbf{u}\|_{\hat{V}} := \|\mathbf{curl} \mathbf{u}\|_2$, see also [3] for the more general case of multiply connected D . Then for $\mathbf{J} \in L^2(D)^3$ the weak formulation reads, find $\mathbf{A} \in \hat{V}$, such that

$$(2.9) \quad \int_D \nu (|\mathbf{curl} \mathbf{A}|) \mathbf{curl} \mathbf{A} \cdot \mathbf{curl} \mathbf{v} \, dx = \int_D \mathbf{J} \cdot \mathbf{v} \, dx, \quad \forall \mathbf{v} \in \hat{V}.$$

Equation (2.9) can be written more compactly, by introducing the vector function $\mathbf{h} : \mathbb{R}^3 \rightarrow \mathbb{R}^3$, $\mathbf{h}(\mathbf{r}) := \nu(|\mathbf{r}|)\mathbf{r}$, as

$$(2.10) \quad \int_D \mathbf{h}(\mathbf{curl} \mathbf{A}) \cdot \mathbf{curl} \mathbf{v} \, dx = \int_D \mathbf{J} \cdot \mathbf{v} \, dx, \quad \forall \mathbf{v} \in \hat{V}.$$

Also, let \hat{V}^* denote the dual space of \hat{V} , by introducing the operator $K : \hat{V} \rightarrow \hat{V}^*$ as

$$(2.11) \quad \langle K\mathbf{u}, \mathbf{v} \rangle := \int_D \mathbf{h}(\mathbf{curl} \mathbf{u}) \cdot \mathbf{curl} \mathbf{v} \, dx,$$

we obtain $\mathbf{A} \in \hat{V}$ as the solution of

$$(2.12) \quad \langle K\mathbf{A}, \mathbf{v} \rangle = (\mathbf{J}, \mathbf{v})_2, \quad \forall \mathbf{v} \in \hat{V}.$$

Existence and uniqueness is guaranteed by the Zarantonello Lemma [54] as (2.6) implies

$$(2.13a) \quad \langle K\mathbf{u}, \mathbf{u} - \mathbf{v} \rangle - \langle K\mathbf{v}, \mathbf{u} - \mathbf{v} \rangle \geq \alpha \|\mathbf{u} - \mathbf{v}\|_{\hat{V}}^2,$$

$$(2.13b) \quad |\langle K\mathbf{u}, \mathbf{w} \rangle - \langle K\mathbf{v}, \mathbf{w} \rangle| \leq 3\beta \|\mathbf{u} - \mathbf{v}\|_{\hat{V}} \|\mathbf{w}\|_{\hat{V}},$$

see [34], i.e., the strong monotonicity and Lipschitz continuity of the nonlinear operator K . Moreover, we have the estimate

$$(2.14) \quad \|\mathbf{A}\|_{\hat{V}} \leq \frac{C_F}{\alpha} \|\mathbf{J}\|_2.$$

REMARK 1. Typically, for the accurate modelling of magnetic devices an interface problem with several materials, e.g., iron and air, has to be studied. Then, the piecewise defined magnetic reluctivity also satisfies (2.6) and the problem is still found to be well-posed, see [10, 31]. Also the extension to multiply connected domains would mainly require a modification of the divergence free condition to ensure the norm equivalence [10]. In the more general case of $f(\mathbf{x}, \cdot)$ with arbitrary x -dependence, $f(\cdot, s)$ must additionally be measurable [53] for all s and consequently 3 + 1-dimensional random fields would occur. However, as our focus lies on the nonlinearity in the stochastic setting, for simplicity, we restrict ourselves to simply connected domains with only one homogeneous nonlinear material.

3. Uncertainties in the Nonlinear Material Law and Stochastic Formulation. Randomness is incorporated, as usual, by introducing a probability space $(\Omega, \mathcal{F}, \mathbb{P})$ and modeling the material law f as a random field $f : \Omega \times \mathbb{R}_0^+ \rightarrow \mathbb{R}_0^+$. A stochastic formulation is based on the following assumption.

ASSUMPTION 2. *The stochastic material law $f(\omega, \cdot)$ satisfies Assumption 1 almost surely (a.s.) with constants α and β independent of ω .*

According to Lemma 2.1 this implies, that the stochastic reluctivity $\nu : \Omega \times \mathbb{R}_0^+ \rightarrow \mathbb{R}^+$, defined as $\nu(\omega, s) := f(\omega, s)/s$, for all $s \in \mathbb{R}^+$ satisfies (2.6) a.s., with constants α, β independent of ω .

Setting for $\mathbf{r} \in \mathbb{R}^3$, $\mathbf{h}(\omega, \mathbf{r}) = \nu(\omega, |\mathbf{r}|) \mathbf{r}$, the stochastic curl-curl problem reads a.s. as

$$(3.1) \quad \int_D \mathbf{h}(\cdot, \mathbf{curl} \mathbf{A}) \cdot \mathbf{curl} \mathbf{v} \, dx = \int_D \mathbf{J} \cdot \mathbf{v} \, dx, \quad \forall \mathbf{v} \in \hat{V}.$$

By Assumption 2 we have a unique solution $\mathbf{A} \in L^p(\Omega, \hat{V})$ for all $p \in \mathbb{N}$ by means of (2.14).

3.1. Random Input Discretization by the Truncated Karhunen–Loève Expansion. In the following we restrict ourselves to an open interval $I \subset \mathbb{R}^+$ and define for f (resp. ν), $\tilde{f} := f|_{\tilde{I}}$. Restricting the uncertainty of the material law to a specific interval is a reasonable assumption in practice and in particular suitable to satisfy the constraints (2.5c) and (2.5d) in the presence of randomness. A globally defined f can be obtained by a differentiable prolongation from I to \mathbb{R}_0^+ .

To be used in computer simulations the input random field $\tilde{f} : \Omega \times \tilde{I} \rightarrow \mathbb{R}^+$ has to be discretized. This is achieved here by introducing the (linear) truncated Karhunen–Loève expansion

$$(3.2) \quad \tilde{f}_M(\omega, s) = \mathbb{E}_{\tilde{f}}(s) + \sum_{n=1}^M \sqrt{\lambda_n} b_n(s) Y_n(\omega).$$

A stronger dependency of \tilde{f}_M w.r.t. Y_n might be obtained by performing a Karhunen–Loève expansion for $\log(\tilde{f})$, rather than f [6]. However, a linear expansion as (3.2) with a moderate number M , might be beneficial in numerical approximations.

We recall the definition of the expected value and covariance function

$$(3.3) \quad \mathbb{E}_{\tilde{f}}(s) := \int_{\Omega} \tilde{f}(\omega, s) \, d\mathbb{P}(\omega),$$

$$(3.4) \quad \text{Cov}_{\tilde{f}}(s, t) := \int_{\Omega} \left(\tilde{f}(\omega, s) - \mathbb{E}_{\tilde{f}}(s) \right) \left(\tilde{f}(\omega, t) - \mathbb{E}_{\tilde{f}}(t) \right) \, d\mathbb{P}(\omega),$$

for $s, t \in \tilde{I}$. Based on the following assumption, some important properties of (3.2) are briefly recalled here, see, e.g., [35, 26, 8, 49].

ASSUMPTION 3. *The image of $Y_n, n = 1, \dots, M$ is uniformly bounded. Additionally, the covariance satisfies $\text{Cov}_{\tilde{f}} \in \mathcal{C}^l(\tilde{I} \times \tilde{I})$, with $l > 2$.*

Consider the self-adjoint and compact operator $T_{\tilde{f}} : L^2(I) \rightarrow L^2(I)$, given by

$$(3.5) \quad (T_{\tilde{f}} u)(s_1) := \int_I \text{Cov}_{\tilde{f}}(s_1, s_2) u(s_2) \, ds_2.$$

Then $(\lambda_n, b_n)_{n=1}^\infty$ are eigenpairs of

$$(3.6) \quad T_{\tilde{f}} u = \lambda u,$$

where the $(b_n)_{n=1}^\infty$ are orthonormal in $L^2(I)$ and $\lambda_1 \geq \lambda_2 \geq \dots \geq 0$. In (3.2), the random variables $(Y_n)_{n=1}^\infty$ subject to

$$(3.7) \quad Y_n = \frac{1}{\sqrt{\lambda_n}} \int_I \left(\tilde{f}(\omega, s) - \mathbb{E}_{\tilde{f}}(s) \right) b_n(s) ds,$$

for $\lambda_n > 0$, are centered and uncorrelated with unit variance. We assume that they are independent and denote their image with Γ_n and set $\Gamma := \prod_{n=1}^M \Gamma_n$.

Approximation properties of (3.2) are well studied, in particular the L^2 -error

$$(3.8) \quad \|\tilde{f} - \tilde{f}_M\|_{L^2(\Omega \times I)}^2 = \sum_{n=M+1}^{\infty} \lambda_n,$$

is optimal among all M -term approximations, see [49]. The remainder in (3.8) can be bounded, investigating the decay rate of the eigenvalues [26, 49]. We obtain

$$(3.9) \quad 0 \leq \lambda_n \leq C n^{-l},$$

with $C > 0$, see [26, Proposition 2.5] and hence,

$$(3.10) \quad \|\tilde{f} - \tilde{f}_M\|_{L^2(\Omega \times I)}^2 \leq C_l M^{1-l}.$$

An analytic covariance yields an exponential decay.

Except for several simple covariance functions, e.g., the exponential kernel, the eigenvalue problem (3.6) has to be solved numerically. This has been addressed, e.g., in [49, 42]. To assure global differentiability, we employ a Galerkin approximation based on a B-spline space. This leads to a generalized discrete eigenvalue problem. Let $I_{\min} := \min(\bar{I})$, $I_{\max} := \max(\bar{I})$, and $q, N \in \mathbb{N}$ and consider a (quasi-uniform) sequence

$$(3.11) \quad I_{\min} = s_0 < s_1 < \dots < s_N = I_{\max},$$

referred to as mesh τ_N . To τ_N we associate the B-spline space $\mathcal{S}_N^{q,k}$ of polynomials of degree q on each sub-interval of τ_N with global continuity $k \in \mathbb{N}$. For the standard iterative construction procedure of B-splines, see, e.g., [24]. The Galerkin approximation of (3.6) reads, following [49, p.111], find $(\lambda_{N,n}, b_{N,n})_{n \geq 1}^\infty \subset \mathbb{R} \times \mathcal{S}_N^{q,k}$ subject to

$$(3.12) \quad \int_I \int_I b_{N,n}(s_1) \text{Cov}_{\tilde{f}}(s_1, s_2) v_N(s_2) ds_1 ds_2 = \lambda_{N,n} \int_I b_{N,n}(s) v_N(s) ds,$$

for all $v_N \in \mathcal{S}_N^{q,k}$. By means of the numerically computed eigenpairs, the discrete Karhunen–Loève expansion reads

$$(3.13) \quad \tilde{f}_{M,N}(\omega, s) = \mathbb{E}_{\tilde{f}}(s) + \sum_{n=1}^M \sqrt{\lambda_{N,n}} b_{N,n}(s) Y_{N,n}(\omega).$$

Based on the approximation properties of B-splines, see, e.g., [30], the Galerkin error contribution can be bounded, following [49], as

$$(3.14) \quad \|\tilde{f}_M - \tilde{f}_{M,N}\|_{L^2(\Omega \times I)}^2 \leq C_M N^{-2(q+1)},$$

with $C_M > 0$ and $q + 1 < l$.

3.2. Application to the Nonlinear Magnetic Material Law. In the following we employ a Karhunen–Loève expansion to discretize the stochastic magnetic material law. We thereby focus on the truncation error, i.e., assume that N is sufficiently large. As in the deterministic case we set $\tilde{f}^{(i)} := \partial_s^i \tilde{f}(\cdot, s)$. To ensure the solvability of the PDE the $L^2(\Omega \times I)$ –convergence of \tilde{f} to \tilde{f}_M is not sufficient and we additionally require that $\tilde{f}_M^{(i)}$ satisfies (1.2).

LEMMA 3.1. *Let Assumption 3 hold true, then there exists $M_0 \in \mathbb{N}$, such that for $M > M_0$*

$$(3.15) \quad \alpha_0 \leq \tilde{f}_M^{(1)}(\omega, s) \leq \beta_0,$$

holds with positive constants α_0, β_0 .

Proof. Based on Assumption 3 it follows by [49, Theorem 2.24] and (3.9), that for $\lambda_n \neq 0$,

$$(3.16) \quad \|\tilde{f}^{(1)}(\omega, \cdot) - \tilde{f}_M^{(1)}(\omega, \cdot)\|_{L^\infty(I)} \leq C_\delta \sum_{n=M+1}^{\infty} \lambda_n^{1/2-\delta} \leq \underbrace{C_{\delta,l} M^{1-l/2+\delta l}}_{=:r_M},$$

a.s., with $0 < \delta < 1/2 - 1/l$ and a positive constant C_δ additionally depending on the covariance and $|\Gamma|$. Hence, the sum on the right-hand-side converges for all M . Moreover, we can choose $M \geq M_0$ large enough such that for almost all $\omega \in \Omega$, $s \in I$,

$$(3.17) \quad \underbrace{\alpha - r_{M_0}}_{=: \alpha_0} \leq \tilde{f}_M^{(1)}(\omega, s) \leq \underbrace{\beta + r_{M_0}}_{=: \beta_0},$$

with $r_{M_0} \in (0, \alpha)$. \square

Let f_M be a continuously differentiable prolongation of \tilde{f}_M from I to \mathbb{R}_0^+ , such that Assumption 2 is satisfied. This can be achieved, e.g., by the construction given in [31]. Then $\nu_M(\omega, s) := f_M(\omega, s)/s$ can be used as material coefficient for the stochastic problem. Complementary to this result, formulas assuring that the shape constraint (3.17) is verified, will be derived in the next section for a concrete setting.

REMARK 2. *We observe that we cannot model f or ν , as normal (or log-normal) random field, as their derivatives would not be bounded uniformly. In particular the trajectories of f would be non-monotonic with a probability greater than zero.*

3.2.1. Practical Realization and Numerical Example. In this section a practical realization under minimal assumptions on f is discussed. Measured data is supposed to be available at equidistant points $I_{\min} \leq \hat{s}_1 < \hat{s}_2 < \dots < \hat{s}_R \leq I_{\max}$. We introduce the table

$$(3.18) \quad \left\{ \left(\hat{s}_i, \hat{f}_{ij} \right), i = 1, \dots, R, j = 1, \dots, Q \right\}$$

and assume that the data is monotonic, i.e., $\hat{f}_{i_1 j} \leq \hat{f}_{i_2 j}$, for $i_1 \leq i_2$ and $j = 1, \dots, Q$. The data is interpolated using \mathcal{C}^1 monotonicity-preserving cubic splines, see [27]. For data with increased oscillations due to measurements a procedure as outlined in [44, 47] should be used.

The situation $Q = 1$ is very common in practice, and additional assumptions on the covariance are needed in this case. To solve the Karhunen–Loève eigenvalue problem, as outlined in Section 3.1, the correlation function

$$(3.19) \quad k_{\tilde{f}}(s, t) = \frac{\text{Cov}_{\tilde{f}}(s, t)}{\sqrt{\text{Cov}_{\tilde{f}}(s, s)} \sqrt{\text{Cov}_{\tilde{f}}(t, t)}},$$

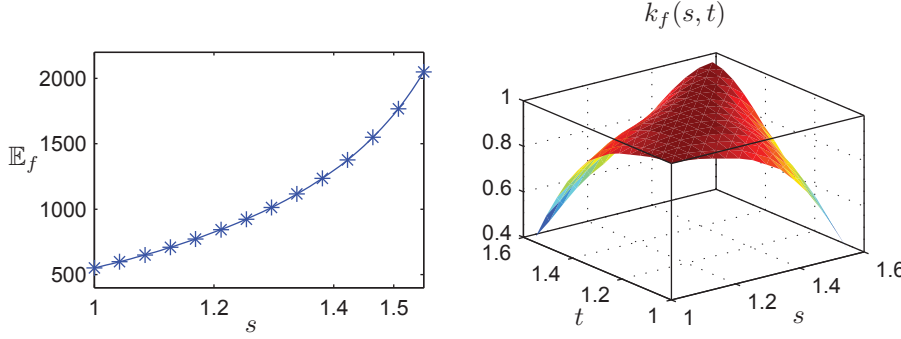


FIG. 2. Expected value \mathbb{E}_f and correlation function k_f for the data given in [45].

is chosen to be approximated by the Gaussian kernel

$$(3.20) \quad k_G(s, t) = \delta^2 e^{-\left(\frac{s-t}{L}\right)^2},$$

where L denotes the correlation length and $\delta > 0$ a parameter. By rescaling with the interpolated sample variance $\left(\text{Var}_{\hat{f}_i}\right)_{i=1}^R$ we obtain the covariance. The associated discrete eigenpairs $(\lambda_n, b_n)_{n=1}^N$ are obtained by discretization with $\mathcal{S}_N^{3,1}$. Then, the random material relation is approximated by

$$(3.21) \quad \tilde{f}_M(\omega, s) = \mathbb{E}_{\tilde{f}}(s) + \delta \sum_{n=1}^M \sqrt{\lambda_n} b_n(s) Y_n(\omega).$$

In (3.21) $\mathbb{E}_{\tilde{f}}$ is obtained by projecting the interpolated sample mean $\left(\mathbb{E}_{\hat{f}_i}\right)_{i=1}^R$ on $\mathcal{S}_N^{3,1}$.

Here, we determine M such that the relative information content satisfies

$$(3.22) \quad \frac{\sum_{n=1}^M \lambda_n}{\sum_{n=1}^{M'} \lambda_n} > 0.95,$$

where $M' \gg M$. For a more rigorous approach to the recovery of the Karhunen–Loève approximation from measured data by means of an a posteriori error analysis, we refer to [5]. Sample realizations of the Y_n can be determined by (3.7), however here, we model them to be distributed uniformly as $\mathbb{U}(-\sqrt{3}, \sqrt{3})$. The parameter δ is used to assure that (3.21) satisfies the shape constraints (3.17), see also [8, p. 1282] for a related discussion in the context of a linear material coefficient. In particular we only need to assure that \tilde{f}_M is monotonic. If $\mathbb{E}_{\tilde{f}}$ can be represented by a spline function, as is the case in the present setting, a simple condition for δ can be derived to this end. To simplify notation let $\eta_M(s) = \sum_{n=1}^M \sqrt{\lambda_n} b_n(s)$ and $\eta_{M,i}$ be obtained by substituting b_n in the previous relation by its i -th spline coefficients. Let $\left(\mathbb{E}_{\tilde{f},i}\right)_{i=1}^N$ denote the coefficient vector of $\mathbb{E}_{\tilde{f}} \in \mathcal{S}_N^{3,1}$. Then from [24] we recall that a sufficient condition for a B-spline to be monotonic is that its coefficients are increasing and hence, monotonicity can be assured by

$$(3.23) \quad \delta < \min_{i=2,\dots,N} \frac{\mathbb{E}_{\tilde{f},i} - \mathbb{E}_{\tilde{f},i-1}}{\sqrt{3}|\eta_{M,i} - \eta_{M,i-1}|},$$

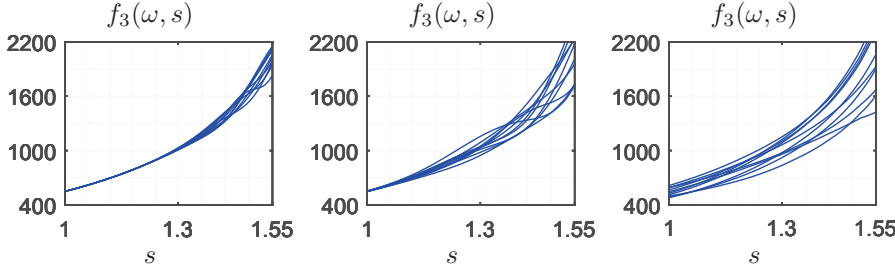


FIG. 3. Ten sample discretizations for $M = 3$, with correlation lengths $L = 1/20$, $L = 1/10$ and $L = 1/2$, respectively. The perturbation amplitudes are $\delta = 0.89$, $\delta = 2.10$ and $\delta = 2.85$, respectively.

where we minimize only over those i with nonzero denominator. In a more general setting one could derive a similar expression by minimizing δ_s given by

$$(3.24) \quad \mathbb{E}_{\tilde{f}}^{(1)}(s) > \delta_s \sqrt{3} |\eta_M^{(1)}(s)|,$$

over all $s \in \bar{I}$.

Let us consider the material uncertainty of an electrical machine. In [45], measured data¹, representing the material properties from twenty-eight machine stator samples ($Q = 28$) from the same production chain was presented. The interval of interest is given by $\bar{I} = [1, 1.55]$ and measurements were taken at $R = 14$ equidistant points. For the given criteria we truncate the Karhunen–Loève expansion with $M = 3$. Figure 2 depicts both the expected value and the correlation function. For illustration we compare the setting for three different correlation lengths $L = 1/20$, $L = 1/10$ and $L = 1/2$, respectively. Figure 3 depicts ten sample realizations for each correlation length, where the coefficient δ is chosen according to (3.23) and a uniform mesh with $N = 60$ spline basis functions is used. It can be readily observed, that a smaller correlation length, corresponding to trajectories with increased oscillations, demands for a smaller δ , i.e., a smaller perturbation magnitude. Also, the largest correlation length $L = 1/2$ gives the best agreement with the measured data and will be chosen in what follows.

3.3. Truncation Error and High-Dimensional Deterministic Problem.

We are now going to investigate the modelling error arising from a finite dimensional noise approximation, i.e., when ν is replaced by ν_M . So far we have explained how this approximation can be achieved by means of the Karhunen–Loève expansion, however, hereafter, we do not restrict ourselves to this specific case anymore. For given ν_M , for $\mathbf{r} \in \mathbb{R}^3$, let $\mathbf{h}_M(\cdot, \mathbf{r}) := \nu_M(\cdot, |\mathbf{r}|) \mathbf{r}$ denote the associated vector function. Then \mathbf{A}_M is defined a.s. as the solution of

$$(3.25) \quad \int_D \mathbf{h}_M(\cdot, \mathbf{curl} \mathbf{A}_M) \cdot \mathbf{curl} \mathbf{v} \, dx = \int_D \mathbf{J} \cdot \mathbf{v} \, dx, \quad \forall \mathbf{v} \in \hat{V}.$$

PROPOSITION 3.2. *Let \mathbf{A} and \mathbf{A}_M be the solution of (3.1) and (3.25), respectively. Moreover, let f as well as f_M satisfy Assumption 2, with constants α, α_0 , respectively. Then we have a.s.*

$$(3.26) \quad \|\mathbf{A} - \mathbf{A}_M\|_{\hat{V}} \leq \|\nu - \nu_M\|_{L^\infty(\mathbb{R}^+)} \frac{C_F \|\mathbf{J}\|_2}{\alpha \alpha_0}.$$

¹The simulation is based on the original data kindly provided by Stéphane Clénet.

Proof. As f satisfies Assumption 2, we have a uniform strong monotonicity property, i.e., a.s.

$$(3.27) \quad \alpha \|\mathbf{A} - \mathbf{A}_M\|_{\hat{V}}^2 \leq \int_D (\mathbf{h}(\cdot, \mathbf{curl} \mathbf{A}) - \mathbf{h}(\cdot, \mathbf{curl} \mathbf{A}_M)) \cdot \mathbf{curl}(\mathbf{A} - \mathbf{A}_M) \, dx$$

and because of equations (3.1) and (3.25) and the Cauchy–Schwarz inequality

$$(3.28) \quad \alpha \|\mathbf{A} - \mathbf{A}_M\|_{\hat{V}} \leq \|\mathbf{h}_M(\cdot, \mathbf{curl} \mathbf{A}_M) - \mathbf{h}(\cdot, \mathbf{curl} \mathbf{A}_M)\|_2.$$

For the right-hand-side we further obtain

$$(3.29) \quad \|\mathbf{h}_M(\cdot, \mathbf{curl} \mathbf{A}_M) - \mathbf{h}(\cdot, \mathbf{curl} \mathbf{A}_M)\|_2$$

$$(3.30) \quad \leq \left(\int_D ((\nu_M(\cdot, |\mathbf{curl} \mathbf{A}_M|) - \nu(\cdot, |\mathbf{curl} \mathbf{A}_M|)) \mathbf{curl} \mathbf{A}_M)^2 \, dx \right)^{1/2}$$

$$(3.31) \quad \leq \|\nu_M - \nu\|_{L^\infty(\mathbb{R}^+)} \|\mathbf{A}_M\|_{\hat{V}}.$$

The result follows from $\|\mathbf{A}_M\|_{\hat{V}} \leq \frac{C_F \|\mathbf{J}\|_2}{\alpha_0}$. \square

Due to (3.26) we have control of the truncation error. For simplicity, this error is omitted in the following, i.e., we assume that the uncertain input has a finite dimensional noise representation:

ASSUMPTION 4. *The random field ν , resp. f , depends (continuously) on M independent random variables solely, i.e., a.s.*

$$(3.32) \quad \nu(\mathbf{Y}(\omega), s) = \nu(\omega, s),$$

where $\mathbf{Y} = (Y_1, Y_2, \dots, Y_M)$.

We recall that \mathbf{Y} may also refer to random variables in closed-form representations of ν or coefficients in spline models, among others. Based on Proposition 3.2 and Assumption 4 it follows from the Doob–Dynkin Lemma [46] (cf. [4]) that we can write

$$(3.33) \quad \mathbf{A}(\mathbf{Y}(\omega), \mathbf{x}) = \mathbf{A}(\omega, \mathbf{x}).$$

We recall that the Y_n have a bounded image and a joint probability density function

$$(3.34) \quad \rho : \Gamma \rightarrow \mathbb{R}^+,$$

such that $\rho(\mathbf{Y}) = \rho_1(Y_1) \rho_2(Y_2) \dots \rho_M(Y_M)$. For all random variables $X \in L_\rho^1(\Gamma)$, such that $X(\omega) = X(\mathbf{Y}(\omega))$ we introduce

$$(3.35) \quad \mathbb{E}[X] = \int_\Gamma X(\mathbf{y}) \rho(\mathbf{y}) \, d\mathbf{y}.$$

We now introduce the following assumption for $f : \Gamma \times \mathbb{R}_0^+ \rightarrow \mathbb{R}_0^+$.

ASSUMPTION 5. *The stochastic material law $f(\mathbf{y}, \cdot)$ satisfies Assumption 1 for ρ -almost all $\mathbf{y} \in \Gamma$, with constants α and β independent of \mathbf{y} .*

The stochastic problem can be recast into a deterministic one with $3 + M$ dimensions.

To this end, let $\hat{\mathcal{V}} := L_\rho^2(\Gamma) \otimes \hat{V}$ be the closure of formal sums $\mathbf{u} = \sum_{i=1}^n v_i \mathbf{w}_i$, where $\{v_i\}_{i=1,n} \subset L_\rho^2(\Gamma)$ and $\{\mathbf{w}_i\}_{i=1,n} \subset \hat{V}$, with respect to the inner product

$$(3.36) \quad (\mathbf{u}, \mathbf{u})_{\hat{\mathcal{V}}} = \mathbb{E} [(\mathbf{u}, \mathbf{u})_{\hat{V}}],$$

cf. [8]. Let $\mathbf{h} : \Gamma \times \mathbb{R}^3 \rightarrow \mathbb{R}^3$. We seek $\mathbf{A} \in \hat{\mathcal{V}}$ such that

$$(3.37) \quad \int_D \mathbf{h}(\mathbf{y}, \mathbf{curl} \mathbf{A}(\mathbf{y})) \cdot \mathbf{curl} \mathbf{v} \, dx = \int_D \mathbf{J} \cdot \mathbf{v} \, dx, \quad \forall \mathbf{v} \in \hat{V},$$

where $\mathbf{A}(\mathbf{y}) := \mathbf{A}(\mathbf{y}, \cdot)$.

4. A Stochastic Collocation Method for the Nonlinear curl–curl Formulation. In the following, the variables $\mathbf{x} \in D$ and $\mathbf{y} \in \Gamma$ will be referred to as deterministic and stochastic variable, respectively. The solution of (3.37) requires discretization in both variables as well as a linearization procedure. To this end, we carry out:

- (i) *deterministic* discretization based on lowest order $\mathcal{H}(\mathbf{curl})$ -conforming finite elements with maximum stepsize h ,
- (ii) *stochastic* discretization based on a collocation procedure on a tensor grid or sparse grid of level q ,
- (iii) l -times iteration of the *linearized* system of equations by means of the Kačanov or Newton–Raphson method.

As we will see in Section 4.4, the use of global, higher order polynomials over Γ is justified by the regularity of the solution, whereas the collocation procedure is particularly attractive for nonlinear problems due to the ease of implementation. We will then proceed by analyzing the approximation error originating from finite element discretization ε_h , stochastic collocation ε_q and linearization ε_l , respectively. By the triangle inequality these errors can be decomposed as

$$(4.1) \quad \|\mathbf{A} - \mathbf{A}_{h,q,l}\|_{\hat{\mathcal{V}}} \leq \underbrace{\|\mathbf{A} - \mathbf{A}_h\|_{\hat{\mathcal{V}}}}_{=:\varepsilon_h} + \underbrace{\|\mathbf{A}_h - \mathbf{A}_{h,q}\|_{\hat{\mathcal{V}}}}_{=:\varepsilon_q} + \underbrace{\|\mathbf{A}_{h,q} - \mathbf{A}_{h,q,l}\|_{\hat{\mathcal{V}}}}_{=:\varepsilon_l}.$$

Additional sources of error can be identified, in particular quadrature errors and the error from numerically solving linear systems of equations. However, these errors will be omitted here. We also claim that all three steps of the proposed scheme commute. This has been shown for the deterministic case in [51] and generalizing to the stochastic collocation method is straightforward.

4.1. Galerkin Finite Element Approximation. Equation (3.37) is approximated in the deterministic variable by the Galerkin finite element method. Higher order schemes are well established and could be employed, however, as our focus lies on the stochastic part, we restrict ourselves to lowest order schemes. We consider discretizations of the Lipschitz polyhedron D with a simplicial mesh \mathcal{T}_h , with maximum size $h > 0$. The mesh is assumed to be quasi-uniform in the sense of [14, Definition 4.4.13], in particular

$$(4.2) \quad \min_{T \in \mathcal{T}_h} \text{diam}(B_T) \geq C_D h,$$

where B_T denotes the largest ball contained in T . We then introduce the discrete spaces

$$(4.3) \quad V_h := \{\mathbf{u} \in V \mid \mathbf{u}|_T = \mathbf{a}_T + \mathbf{b}_T \times \mathbf{x}, \quad \mathbf{a}_T, \mathbf{b}_T \in \mathbb{R}^3, \quad \forall T \in \mathcal{T}_h\},$$

$$(4.4) \quad W_h := \{v \in \mathcal{H}_0^1(D) \mid v|_T = \mathbf{a}_T \cdot \mathbf{x} + b_T, \quad \mathbf{a}_T \in \mathbb{R}^3, b_T \in \mathbb{R}, \quad \forall T \in \mathcal{T}_h\},$$

i.e., V_h and W_h are spanned by lowest order Nédélec and Lagrange elements, respectively. As in the continuous case, the space of (discrete) divergence free functions, is introduced as

$$(4.5) \quad \hat{V}_h := \{\mathbf{u}_h \in V_h \mid (\mathbf{u}_h, \mathbf{grad} v_h)_2 = 0, \quad \forall v_h \in W_h\}.$$

We observe that \hat{V}_h is not a subspace of \hat{V} , as (weak) discrete divergence free functions are not (weak) divergence free in general. The deterministic finite element approximation consists in computing $\mathbf{A}_h : \Gamma \rightarrow \hat{V}_h$ such that for ρ -almost all $\mathbf{y} \in \Gamma$,

$$(4.6) \quad \int_D \mathbf{h}(\mathbf{y}, \mathbf{curl} \mathbf{A}_h(\mathbf{y})) \cdot \mathbf{curl} \mathbf{v}_h \, dx = \int_D \mathbf{J} \cdot \mathbf{v}_h \, dx, \quad \forall \mathbf{v}_h \in \hat{V}_h,$$

holds. Existence and uniqueness can be established based on a discrete Poincaré–Friedrichs inequality [32, Theorem 4.7], see, e.g., [53].

4.2. Stochastic Collocation Method. Stochastic discretization is based on a collocation approach using either a tensor or a sparse grid, see, e.g., [52, 6, 7, 38]. Starting with the (isotropic) tensor grid, following [38], the collocation points are given as

$$(4.7) \quad H_{q,M}^T := \{y_1^1, y_1^2, \dots, y_1^{n(q)}\} \times \{y_2^1, y_2^2, \dots, y_2^{n(q)}\} \times \dots \times \{y_M^1, y_M^2, \dots, y_M^{n(q)}\},$$

where in each dimension $m = 1, \dots, M$, we have $n(q) = p(q) + 1$ collocation points and $N_q = n(q)^M$ in total. Note that p refers to the underlying polynomial degree, which we identify with the level for the tensor grid case as $p(q) = q$. Also, a global index k is associated to the local indices in the usual way [7]. The collocation points are chosen as the roots of the orthogonal polynomials associated to the probability density function ρ . As commonly done [39, 7] we introduce the notation $\mathbf{y} = (y_m, \hat{\mathbf{y}}_m)$, $\hat{\mathbf{y}}_m = (y_1, \dots, y_{m-1}, y_{m+1}, \dots, y_M)$. Let $\mathcal{Q}_p(\Gamma_m)$ be the space of polynomials of degree at most p in Γ_m . Then we introduce in each dimension the one-dimensional Lagrange interpolation operator $I_p^m : \mathcal{C}(\Gamma_m; V) \rightarrow \mathcal{Q}_p(\Gamma_m) \otimes V$ such that

$$(4.8) \quad I_p^m \mathbf{u}(\mathbf{y}) = \sum_{i=1}^{p+1} \mathbf{u}(y_m^i, \hat{\mathbf{y}}_m) l_m^i(y_m),$$

where $l_m^i(y_m)$ is the Lagrange polynomial of degree p associated to the point y_m^i . The tensor grid interpolation formula reads as

$$(4.9) \quad \mathcal{I}_{q,M} \mathbf{u}(\mathbf{y}) = I_{p(q)}^1 \otimes \dots \otimes I_{p(q)}^M \mathbf{u}(\mathbf{y}) = \sum_{k=1}^{N_q} \mathbf{u}(\mathbf{y}_k) l_k(\mathbf{y}),$$

where $l_k(\mathbf{y})$ is the global Lagrange polynomial associated to the point $\mathbf{y}_k \in H_{q,M}^T$.

An isotropic tensor grid, with n points in each direction, can only be used for moderate dimensions M , as the total number of collocation points grows as n^M . Therefore, collocation in higher dimensions is based on sparse grids [13, 41]. For simplicity we consider isotropic Smolyak grids, solely. Anisotropic sparse grids are discussed, e.g., in [40]. Following [38], let $\mathbf{j} \in \mathbb{N}_0^M$ be a multi-index and

$$(4.10) \quad \mathcal{I}_{\mathbf{j},M} \mathbf{u}(\mathbf{y}) = \sum_{i_1=1}^{p(j_1)+1} \dots \sum_{i_M=1}^{p(j_M)+1} \mathbf{u}\left(y_{1,j_1}^{i_1}, \dots, y_{M,j_M}^{i_M}\right) \prod_{m=1}^M l_{m,j_m}^{i_m}(y_m),$$

the associated multi-dimensional Lagrange interpolation operator, where the Gauß knots $\{y_{m,j_m}^{i_m}\}_{i_m=1}^{p(j_m)+1}$ and the Lagrange polynomials $\{l_{m,j_m}^{i_m}\}_{i_m=1}^{p(j_m)+1}$ now also depend on the multi-index \mathbf{j} . For the choice $p(j) = 2^j$ for $j > 0$ and $p(0) = 0$, the Smolyak formula is given by

$$(4.11) \quad \mathcal{A}_{q,M} \mathbf{u}(\mathbf{y}) = \sum_{q-M+1 \leq |\mathbf{j}|_1 \leq q} (-1)^{q-|\mathbf{j}|_1} \binom{M-1}{q-|\mathbf{j}|_1} \mathcal{I}_{\mathbf{j},M} \mathbf{u}(\mathbf{y}).$$

The associated sparse grid is denoted $H_{q,M}^S$. Evaluating (4.9) and (4.11) requires solving

$$(4.12) \quad \int_D \mathbf{h}(\mathbf{y}_k, \mathbf{curl} \mathbf{A}_h(\mathbf{y}_k)) \cdot \mathbf{curl} \mathbf{v}_h \, dx = \int_D \mathbf{J} \cdot \mathbf{v}_h \, dx, \quad \forall \mathbf{v}_h \in \hat{V}_h,$$

for all collocation points \mathbf{y}_k in $H_{q,M}^T$ and $H_{q,M}^S$, respectively.

4.3. Linearization. At each collocation point, iterative linearization is carried out until the linearization error is found to be sufficiently small. The l -th iterate, $l \in \mathbb{N}$, consists in computing $\mathbf{A}_{h,q,l} \in \mathcal{Q}_q(\Gamma) \otimes \hat{V}_h$ such that for $k = 1, \dots, N_q$

$$(4.13) \quad \int_D \mathbf{h}_L(\mathbf{y}_k, \mathbf{curl} \mathbf{A}_{h,q,l}(\mathbf{y}_k)) \cdot \mathbf{curl} \mathbf{v}_h \, dx = \int_D \mathbf{J} \cdot \mathbf{v}_h \, dx, \quad \forall \mathbf{v}_h \in \hat{V}_h,$$

where $\mathcal{Q}_q(\Gamma)$ refers to the polynomial space associated either to tensor or to Smolyak interpolation. For a precise definition of these spaces, see, e.g., [7]. The representation (4.13) follows [25, 16] and in particular we consider the linearization,

$$(4.14) \quad \mathbf{h}_L(\cdot, \mathbf{r}) = \nu(\cdot, |\mathbf{r}_{l-1}|) \mathbf{r},$$

for $\mathbf{r}, \mathbf{r}_{l-1} \in \mathbb{R}^3$. This is usually referred to as Kačanov method or successive substitution in the literature. Note that the case of the Newton–Raphson method, i.e.,

$$(4.15) \quad \mathbf{h}_L(\cdot, \mathbf{r}) = \nu(\cdot, |\mathbf{r}_{l-1}|) \mathbf{r} + \frac{\nu^{(1)}(\cdot, |\mathbf{r}_{l-1}|)}{|\mathbf{r}_{l-1}|} \mathbf{r}_{l-1} \otimes \mathbf{r}_{l-1} (\mathbf{r} - \mathbf{r}_{l-1}),$$

is also covered. Under restrictions on the starting point $\mathbf{A}_{h,q,0}$ and damping, if necessary, $\mathbf{A}_{h,q,l}$ converges to $\mathbf{A}_{h,q}$. At each step equation (4.13) is well-posed by the Lax–Milgram Lemma for both choices. For the Kačanov method, this follows by observing that

$$\nu(\mathbf{y}, |\mathbf{curl} \mathbf{A}_{l-1}|) \in [\alpha, \beta].$$

For the Newton–Raphson method we refer to Lemma 4.1 below.

4.4. Stochastic Regularity and Convergence Analysis. Convergence of the stochastic collocation method introduced above, can be established once the regularity of the solution is known. Whereas for the present nonlinear elliptic problem, the regularity w.r.t. the deterministic variable \mathbf{x} is well known, to our knowledge, the stochastic regularity of the solution \mathbf{A} w.r.t. \mathbf{y} has not been investigated. In the case of a linear elliptic PDE it is well known, that under some mild assumptions the

solution is an analytic function of the stochastic variable [7, 39, 23]. Similar results hold true for several types of nonlinear problems, see [19, 20]. Here, the mapping

$$(4.16) \quad \mathbf{y} \mapsto \nu(\cdot, |\mathbf{curl} \mathbf{A}(\mathbf{y})|)$$

is real, but not complex differentiable, see [33, 10], and this impedes a complex analysis. Moreover, the techniques presented in [19], based on the implicit function theorem, cannot be applied as a norm gap arises. More precisely, the nonlinearity $\mathbf{h} : L^p(D)^3 \rightarrow L^q(D)^3$ can be differentiated only for $q < p$, see [50]. Higher order differentiability even requires a larger difference between p and q . Therefore, we conduct an explicit higher order sensitivity analysis to precisely determine the stochastic regularity.

We define $\nu_\gamma(\mathbf{y}, |\mathbf{r}|) := \partial_{\mathbf{y}}^\gamma \nu(\mathbf{y}, |\mathbf{r}|)$, $\mathbf{h}_\gamma(\mathbf{y}, \mathbf{r}) := \partial_{\mathbf{y}}^\gamma \mathbf{h}(\mathbf{y}, \mathbf{r})$ and $\mathbf{A}_\gamma := \partial_{\mathbf{y}}^\gamma \mathbf{A}(\mathbf{y})$, respectively. We will encounter derivatives of the function $\mathbf{h}(\cdot, \mathbf{r}) = \nu(\cdot, |\mathbf{r}|) \mathbf{r}$ with respect to \mathbf{r} , i.e., multi-linear maps $D_{\mathbf{r}}^k \mathbf{h}(\cdot, \mathbf{r}) : \mathbb{R}^{3k} \rightarrow \mathbb{R}^3$. Of particular interest is the Jacobian $D_{\mathbf{r}}^1 \mathbf{h}$, identified with the differential reluctivity tensor as

$$(4.17) \quad \nu_d(\mathbf{y}, \mathbf{r}) := \begin{cases} \nu(\mathbf{y}, |\mathbf{r}|) + \frac{\nu^{(1)}(\mathbf{y}, |\mathbf{r}|)}{|\mathbf{r}|} \mathbf{r} \otimes \mathbf{r}, & \mathbf{r} \neq 0, \\ \nu(\mathbf{y}, 0), & \mathbf{r} = 0. \end{cases}$$

An important property is stated in the following Lemma.

LEMMA 4.1. *Let Assumption 5 hold true. Then the differential reluctivity tensor satisfies*

$$(4.18a) \quad |\nu_d(\mathbf{y}, \mathbf{s})| \leq \beta_d,$$

$$(4.18b) \quad \mathbf{r}^\top \nu_d(\mathbf{y}, \mathbf{s}) \mathbf{r} \geq \alpha_d |\mathbf{r}|^2,$$

for $\alpha_d, \beta_d > 0$ and all $\mathbf{y} \in \mathbb{R}^M$, $\mathbf{r}, \mathbf{s} \in \mathbb{R}^3$.

Proof. This result has been established, e.g., in [34, Lemma 3.1]. \square

In particular this implies, that the bilinear form $b_d(\mathbf{u}; \cdot, \cdot)$, defined by

$$(4.19) \quad b_d(\mathbf{u}; \mathbf{v}, \mathbf{w}) := \int_D \nu_d(\cdot, \mathbf{curl} \mathbf{u}) \mathbf{curl} \mathbf{v} \cdot \mathbf{curl} \mathbf{w} dx,$$

is continuous and coercive on \hat{V} . We recall that \hat{V}_h is not a subspace of \hat{V} . However, b_d is continuous and coercive on \hat{V}_h , too. The form b_d arises naturally when sensitivities are computed and also in the linearized system obtained by the Newton–Raphson method, which is well-posed at each iteration step by the properties just established.

Provided that f is k -times differentiable, the question arises whether higher order derivatives of the solution exist as well. In a first step, we consider the case $k \leq 3$. We impose the following assumption on the material law.

ASSUMPTION 6. *For the parametric material law there holds*

$$(4.20) \quad f \in \mathcal{C}^3(\Gamma \times \mathbb{R}^+)$$

with bounded and uniformly continuous derivatives, and additionally

$$f^{(2)}(\cdot, 0) = f^{(3)}(\cdot, 0) = 0.$$

The vanishing higher order derivatives of f around the origin are used here to ensure differentiability in presence of the absolute value. Under the previous assumption we infer that $D_{\mathbf{r}}^k \mathbf{h}$ is bounded.

LEMMA 4.2. *Let Assumption 6 hold true. Then for $|\alpha|_1 \leq k \leq 3$, $\partial_{\mathbf{r}}^\alpha h_j$ is continuous and $|\partial_{\mathbf{r}}^\alpha h_j| \leq C_k$.*

Proof. For $\mathbf{r} \neq 0$, as $h_j(\cdot, \mathbf{r}) = f(\cdot, |\mathbf{r}|)r_j/|\mathbf{r}|$ we see that h_j is k -times continuously differentiable. Hence, if $\partial_{\mathbf{r}}^\alpha h_j(\cdot, \mathbf{r})$ is bounded for $\mathbf{r} \rightarrow \infty$ and $\mathbf{r} \rightarrow 0$ the result follows. For $\mathbf{r} \rightarrow \infty$ we observe that $f^{(k)}$ is bounded (by Assumption 6) and that the same holds true for $\partial_{\mathbf{r}}^\alpha(\mathbf{r}/|\mathbf{r}|)$.

For $\mathbf{r} \rightarrow 0$ we first observe that by the rule of l'Hôpital

$$(4.21) \quad \nu^{(k-1)}(\cdot, 0) = f^{(k)}(\cdot, 0)/k$$

and hence $\nu^{(1)}(\cdot, 0) = \nu^{(2)}(\cdot, 0) = 0$ by Assumption 6. Hence, using the expressions for $D_{\mathbf{r}}^k \mathbf{h}$ given in Appendix A we infer that $D_{\mathbf{r}}^1 \mathbf{h}(\cdot, 0)(\mathbf{s}_1) = \nu(\cdot, 0)\mathbf{s}_1$ and that $D_{\mathbf{r}}^2 \mathbf{h}(\cdot, 0) = D_{\mathbf{r}}^3 \mathbf{h}(\cdot, 0) = 0$. \square

By examining the proof of Lemma 4.2 we observe that if $|\beta|_1 \leq k$, $D_{\mathbf{r}}^{k-|\beta|_1} \mathbf{h}_\beta$ is bounded, too.

In the continuous case, formally differentiating the strong form of the boundary value problem, we obtain for the derivative \mathbf{A}_γ

$$(4.22a) \quad \mathbf{curl}(\nu_d(\cdot, \mathbf{curl} \mathbf{A}) \mathbf{curl} \mathbf{A}_\gamma) = \mathbf{curl} \mathbf{F}_k \left((\mathbf{A}_\alpha)_{\alpha < \gamma} \right),$$

$$(4.22b) \quad \operatorname{div} \mathbf{A}_\gamma = 0,$$

$$(4.22c) \quad \mathbf{A}_\gamma \times \mathbf{n} = 0,$$

where, as shown in the Appendix, \mathbf{F}_k is given by

$$(4.23) \quad \mathbf{F}_k = - \sum_{0 \leq \alpha \leq \gamma} \binom{\gamma}{\alpha} \sum_{\pi \in \Pi^*} D_{\mathbf{r}}^{\operatorname{ca}(\pi)} \mathbf{h}_\alpha(\cdot, \mathbf{curl} \mathbf{A}) (\mathbf{curl} \mathbf{A}_{\pi_1}, \dots, \mathbf{curl} \mathbf{A}_{\pi_{\operatorname{ca}(\pi)}}).$$

With Π^* we denote the set of partitions of $\gamma - \alpha$, such that $\operatorname{ca}(\pi) > 1$ if $\alpha = 0$, where $\operatorname{ca}(\pi)$ refers to the cardinality of π . We refer to Appendix B for a more detailed definition of the underlying sets of \mathbf{F}_k . We observe, that $\pi_i < \gamma$ for $i = 1, \dots, \operatorname{ca}(\pi)$ and hence the derivatives contained in the right-hand-side are of lower order. Equation (4.22) is the basis for establishing the regularity of the solution with respect to the stochastic variable. This in turn determines the convergence rate of the corresponding discretization error. Before bounding the collocation error, we discuss the finite element error. To this end, we assume the following:

ASSUMPTION 7. *The solution of (3.37) has the additional regularity $\mathbf{A} \in L^\infty(\Gamma, \mathcal{H}^s(\mathbf{curl}; D))$, with $s \in (1/2, 1]$, and the same holds true for the weak solution of (4.22), if it exists.*

Based on this regularity assumption, we can establish the following result:

LEMMA 4.3. *Let Assumptions 5 and 7 hold true, then the deterministic error is bounded as*

$$(4.24) \quad \varepsilon_h \leq Ch^s,$$

where C depends on \mathbf{A} and on s but is independent of \mathbf{y} .

Proof. For the deterministic error ε_h , also in the present nonlinear case, Céa's Lemma

$$(4.25) \quad \|\mathbf{A}(\mathbf{y}) - \mathbf{A}_h(\mathbf{y})\|_{\hat{V}} \leq C_1 \inf_{\mathbf{v}_h \in \hat{V}_h} \|\mathbf{A}(\mathbf{y}) - \mathbf{v}_h\|_{\hat{V}},$$

holds for ρ -almost all $\mathbf{y} \in \Gamma$, see [10]. Then from [37, Theorem 5.41] we obtain

$$(4.26) \quad \|\mathbf{A}(\mathbf{y}) - \Pi_h \mathbf{A}(\mathbf{y})\|_{\hat{V}} \leq C_2 h^s \|\mathbf{A}(\mathbf{y})\|_{\mathcal{H}^s(\mathbf{curl}; D)},$$

where Π_h is the canonical interpolation operator [37, p. 134] and the constant C_2 depends on s , but is independent of \mathbf{y} . As $\mathbf{A} \in L^\infty(\Gamma, \mathcal{H}^s(\mathbf{curl}; D))$, we conclude that $\varepsilon_h \leq C_3 h^s$. \square Based on the sensitivity analysis carried out in this section, we can now use Theorems 4 and 5 of [38] to establish the main result.

THEOREM 4.4. *Let Assumptions 5, 6 and 7 hold true. There holds*

$$(4.27) \quad \|\mathbf{A} - \mathbf{A}_{h,q}\|_{\hat{V}} \leq C h^s + \varepsilon_q,$$

where C is the constant from Lemma 4.3. Moreover, let i_s be an integer $1 \leq i_s \leq k$, such that $i_s = 1$ for $s \in (1/2, 3/4)$, $i_s = 2$ for $s \in [3/4, 1)$ and $i_s = 3$ for $s = 1$, respectively. For the isotropic tensor grid collocation method we have

$$(4.28) \quad \varepsilon_q \leq \begin{cases} C_T q^{-i_s}, \\ \frac{C_T}{2} N_q^{-i_s/M}, \end{cases}$$

with respect to the level (polynomial degree) q and the number of collocation points N_q , respectively. For the sparse grid collocation method and $M \leq i_s$, there holds

$$(4.29) \quad \varepsilon_q \leq \begin{cases} C_S (q+1)^{2M} 2^{-\lfloor i_s/M \rfloor (q+1)}, \\ C_S \left(1 + \log_2 \left(\frac{N_q}{M}\right)\right)^{2M} N_q^{-\lfloor i_s/M \rfloor \frac{\log 2}{\xi + \log M}}, \end{cases}$$

with respect to the level q and the number of collocation points N_q in the sparse grid, respectively. The constants C_T, C_S depend on s, \mathbf{A}, ν, ρ and $\xi \approx 2.1$.

Proof. The deterministic error estimate has been established in Lemma 4.3. In a first step, we bound the stochastic collocation error for the isotropic tensor grid. In this case, the collocation error can be recast as an interpolation error

$$(4.30) \quad \mathbf{A}_h - \mathbf{A}_{h,q} = \mathbf{A}_h - \mathbf{I}_q \mathbf{A}_h.$$

We will consider the case $M = 1$, solely, as the result for $M > 1$ follows by induction, see, e.g., [15, Lemma 7.1] or [38, Theorem 4]. The collocation error is related to the best-approximation error in $\mathcal{Q}_q(\Gamma) \otimes \hat{V}_h$, following [7], as

$$(4.31) \quad \|\mathbf{A}_h - \mathbf{I}_q \mathbf{A}_h\|_{L^2_\rho(\Gamma) \otimes \hat{V}} \leq C_1 \inf_{\mathbf{v} \in \mathcal{Q}_q(\Gamma) \otimes \hat{V}_h} \|\mathbf{A}_h - \mathbf{v}\|_{L^\infty(\Gamma, \hat{V})}.$$

The error decay then depends on the smoothness of \mathbf{A} (and hence \mathbf{A}_h) with respect to the stochastic variable. We note that, as $M = 1$, $\partial_{\mathbf{y}}^\gamma \mathbf{A}$ simplifies to $\partial_y^{i_s} \mathbf{A}$. Using (4.22) and the coercivity of b_d we can formally bound

$$(4.32) \quad \|\partial_y^{i_s} \mathbf{A}\|_{\hat{V}} \leq C_2 \|\mathbf{F}_{i_s}\|_2.$$

Applying the generalized Hölder inequality and Lemma 4.2 yields

$$\begin{aligned} \|\mathbf{F}_{i_s}\|_2 &\leq C_3 \max_{\pi} \|\partial_{\mathbf{y}}^{\pi^1} \mathbf{curl} \mathbf{A} \cdots \partial_{\mathbf{y}}^{\pi^{\text{ca}(\pi)}} \mathbf{curl} \mathbf{A}\|_2 \\ &\leq C_3 \max_{\pi} \|\partial_{\mathbf{y}}^{\pi^1} \mathbf{curl} \mathbf{A}\|_{L^p(D)^3} \cdots \|\partial_{\mathbf{y}}^{\pi^{\text{ca}(\pi)}} \mathbf{curl} \mathbf{A}\|_{L^p(D)^3}, \end{aligned}$$

where $p/2 = \text{ca}(\pi) \leq i_s$ and C_3 depends on ν and s . Hence, we have to choose i_s such that $\partial_y^j \mathbf{curl} \mathbf{A}(y) \in L^{2i_s}(D)^3$, for $j = 0, \dots, i_s - 1$ and ρ -almost all $y \in \Gamma$:

- (i) For $s \in (1/2, 3/4)$ we obtain $i_s = 1$ as we only have $\mathbf{curl} \mathbf{A}(y) \in L^2(D)^3$.
- (ii) For $s \in [3/4, 1)$ we can set $i_s = 2$ as $\partial_y^j \mathbf{curl} \mathbf{A}(y) \in L^4(D)^3$ holds, for $j = 0, 1$.

This follows from the Sobolev embedding theorem, see, e.g. [37, Theorem 3.7],

as we have $\partial_y^j \mathbf{curl} \mathbf{A}(y) \in \mathcal{H}^s(D)^3$.

- (iii) For $s = 1$ we obtain $i_s = 3$, as we can show that $\partial_y^j \mathbf{curl} \mathbf{A}(y) \in L^6(D)^3$, for $j = 0, 1, 2$

using again the Sobolev embedding theorem.

Hence, the results of Jackson quoted from [38] yield

$$(4.33) \quad \|\mathbf{A}_h - \mathbf{I}_q \mathbf{A}_h\|_{L^2_\rho(\Gamma) \otimes \hat{V}} \leq C_4 q^{-i_s} \max_{j=0, \dots, i_s} \|\partial_y^j \mathbf{A}_h\|_{L^\infty(\Gamma, \hat{V})}$$

with C_4 depending on s and by induction for $M > 1$

$$(4.34) \quad \varepsilon_q \leq C_5 q^{-i_s} \sum_{m=1}^M \max_{j=0, \dots, i_s} \|\partial_{y_m}^j \mathbf{A}_h\|_{L^\infty(\Gamma, \hat{V})} \leq C_6 q^{-i_s}.$$

The results for the sparse grid collocation error can be inferred from [38] or [13] once bounds on mixed derivatives of order k , i.e., $\partial_y^\gamma \mathbf{A}$ with $|\gamma| \leq k$ for $j = 1, \dots, M$ have been established. Using the same arguments as above we obtain

$$(4.35) \quad \|\partial_y^\gamma \mathbf{A}\|_{\hat{V}} \leq C_7 \|\mathbf{F}_{|\gamma|_1}\|_2$$

for $|\gamma|_1 \leq i_s$. This in turn ensures bounded mixed derivatives of order $k = \lfloor i_s/M \rfloor$ for the case $M \leq i_s$, solely. Then the results follow from Theorem 5 of [38]. \square

REMARK 3. *Concerning the stochastic discretization error, in the two-dimensional case we can choose $i_s = 2$ for $s \in [1/2, 2/3)$ and $i_s = 3$ for $s \in [2/3, 1]$, respectively.*

REMARK 4. *The linearization error could be included into this convergence estimate: provided that the initial values $\mathbf{A}_{h,q,0}(\mathbf{y}_k)$ are sufficiently close to $\mathbf{A}_{h,q}(\mathbf{y}_k)$, there exists $r \in (0, 1)$, such that*

$$(4.36) \quad \varepsilon_l \leq C r^l$$

for the linearization error of the solution $\mathbf{A}_{h,q,l}$ of (4.13) obtained by the Kačanov method. An improved estimate could be obtained for the Newton–Raphson method.

REMARK 5. *The sparse grid convergence rate of $\mathcal{O}(N_q^{-\gamma \lfloor i_s/M \rfloor})$, with $\gamma \in (0, 1)$, is smaller than the tensor grid convergence rate of $\mathcal{O}(N_q^{-i_s/M})$. This reduction, due to a lack of mixed regularity of the solution, is also observed in the numerical experiments in Section 5. However, for smooth solutions the sparse grid approach is expected to be more efficient for large M .*

We now address the question whether a fast convergence, e.g., a rate of q^{-k} for the tensor grid and arbitrary $k \in \mathbb{N}$, can be obtained under suitable regularity assumptions on the material input data. This is true if $\mathbf{curl} \mathbf{A}$ is bounded uniformly, e.g., for smooth domains and data, as can be seen by the preceding arguments. Also, if we accept a non-uniform constant with respect to the mesh size h , the decay of the stochastic discretization error can be improved, as stated in the following.

PROPOSITION 4.5. *Let Assumption 5 hold true and let $\partial_{\mathbf{r}}^\alpha \partial_{\mathbf{y}}^\beta \mathbf{h}$ be continuous and bounded, for $|\alpha|_1 + |\beta|_1 \leq k \in \mathbb{N}$. Then we have*

$$(4.37) \quad \varepsilon_q \leq C_{T,h,k} q^{-k},$$

for a tensor grid and

$$(4.38) \quad \varepsilon_q \leq C_{S,h,k} (q+1)^{2M} 2^{-\lfloor k/M \rfloor (q+1)},$$

if $M \leq k$, for a sparse grid, respectively. The constants additionally depends on \mathbf{A}, ν, ρ .

Proof. As in the proof of Theorem 4.4 we bound \mathbf{F}_k as

$$(4.39) \quad \|\mathbf{F}_k\|_2 \leq C_k \max_{\pi} \left\| |\mathbf{curl} \partial_{\mathbf{y}}^{\pi_1} \mathbf{A}_h| \cdots |\mathbf{curl} \partial_{\mathbf{y}}^{\pi_{\text{ca}(\pi)}} \mathbf{A}_h| \right\|_2$$

$$(4.40) \quad \leq \tilde{C}_k h^{-k/2} \max_{\pi} \|\partial_{\mathbf{y}}^{\pi_1} \mathbf{A}_h\|_{\hat{V}} \cdots \|\partial_{\mathbf{y}}^{\pi_{\text{ca}(\pi)}} \mathbf{A}_h\|_{\hat{V}},$$

where we have used

$$(4.41) \quad \|\mathbf{curl} \partial_{\mathbf{y}}^{\pi_i} \mathbf{A}_h\|_{L^\infty(D)^3} \leq h^{-1/2} \|\mathbf{curl} \mathbf{A}_h\|_2,$$

by the shape-uniformity of the mesh (4.2). This yields

$$(4.42) \quad \|\partial_{\mathbf{y}}^{\gamma} \mathbf{A}_h\|_{\hat{V}} \leq C_{k,h} \|\mathbf{A}_h\|_{\hat{V}},$$

with $|\gamma|_1 = k$, for the solution $\mathbf{A}_h(\mathbf{y})$ of (4.6). The result can now be established along the lines of the proof of Theorem 4.4 by observing that (4.33) holds true for k arbitrary. \square

A similar idea was applied in [43] in a two-dimensional setting to establish the Lipschitz continuity of the Newton operator.

5. Numerical Examples. Several numerical examples are presented here to illustrate the findings. In 2D we consider a stochastic version of the p -Laplacian, where the solution is known exactly, and the L-shaped domain, respectively. In 3D the magnetostatic TEAM benchmark problem 13 [2] will be discussed with the stochastic material law of Section 3.2.1. Here, numerical results are obtained using FEniCS [51], and all non-uniform meshes are generated by Gmsh [28]. Tensor and sparse grids are generated using the Sparse grids Matlab kit [11, 1].

In 2D, the curl operator reduces to $\mathbf{curl}(u \mathbf{e}_3) = (\partial_{x_2} u, -\partial_{x_1} u, 0)$, where \mathbf{e}_3 denotes the unit vector in the third dimension. The 2D equivalent of (2.9) then reads, find $u \in \mathcal{H}_0^1(D)$ subject to

$$(5.1) \quad (\nu(|\mathbf{grad} u|) \mathbf{grad} u, \mathbf{grad} v)_2 = (J, v)_2 \quad \forall v \in \mathcal{H}_0^1(D).$$

Equation (5.1) is approximated by means of W_h , i.e., lowest order nodal finite elements.

5.1. p -Laplace. We consider $D = (0, 1) \times (0, 1)$, a constant current $J = 2$ and for $s \in \mathbb{R}^+$

$$(5.2) \quad \nu(s) = s^{p-2},$$

giving rise to the p -Laplace problem considered in [25]. The solution is given by

$$(5.3) \quad u(p, (x_1, x_2)) = -\frac{p-1}{p} |(x_1, x_2) - (0.5, 0.5)|^{\frac{p}{p-1}} + \frac{p-1}{p} 0.5^{\frac{p}{p-1}},$$

as we use the inhomogeneous Dirichlet boundary condition $u|_{\partial D}$. Modeling $Y = p$ as a single random parameter, with $Y > 1$ a.s., we obtain a stochastic problem. For

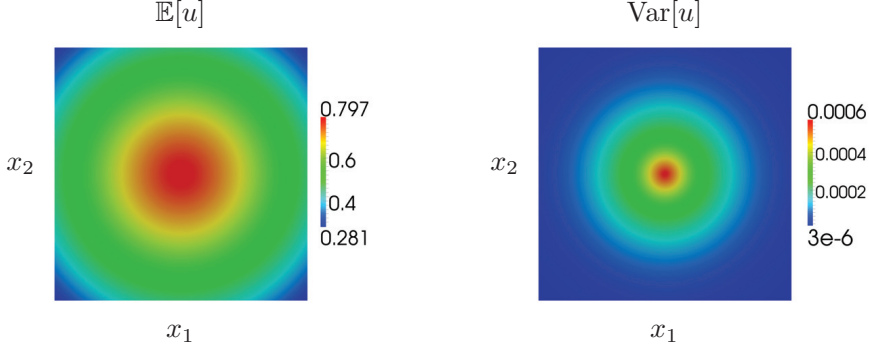


FIG. 4. p -Laplace example. Left: $\mathbb{E}_u(x_1, x_2)$ of analytic solution. Right: $\text{Var}_u(x_1, x_2)$ of analytic solution.

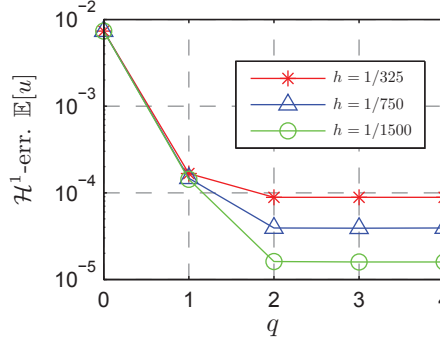


FIG. 5. p -Laplace example. Discretization error, i.e., \mathcal{H}^1 -error of the expected value for different levels of spatial discretization and small linearization error. A fast error convergence is observed until the spatial discretization error level is attained. As a reference, $\mathbb{E}[u]$ is approximated with $\mathbb{E}_q[u]$, $q = 10$.

each Y we have $u(Y, \cdot) \in \mathcal{H}^1(D)$ and even $\mathbf{grad} u(Y, \cdot) \in L^\infty(D)^2$. Hence, we expect a fast spectral stochastic convergence. Note that (5.2) violates the assumptions on the reluctivity for $s \rightarrow \{0, \infty\}$. However, monotonicity and continuity results can be obtained as outlined in [17]. We model Y as uniformly distributed on $(3, 5)$, i.e., $Y \sim \mathbb{U}(3, 5)$. Using a uniform triangulation, (5.1) is iteratively solved by means of the Kačanov method (with damping) until the solution increment is below 10^{-12} in the discrete L^∞ -norm, which yields a negligible linearization error compared to the other sources of error. In Figure 4 we depict the expected value and variance of the solution, respectively. In Figure 5 the error $\|\mathbb{E}[u - u_{q,h}]\|_{\mathcal{H}_0^1(D)}$ is depicted for different values of h . As we are not aware of a closed form solution of $\mathbb{E}[u]$, we approximate it by $\mathbb{E}_q[u]$, with $q = 10$. From Figure 5 an exponential decay of the stochastic error can be observed until the corresponding discretization error level is attained.

5.2. L-Shaped Domain. Another two-dimensional example is the L-shaped domain, given by $[-1, 1]^2 \setminus [0, 1]^2$. Homogeneous Dirichlet boundary conditions are

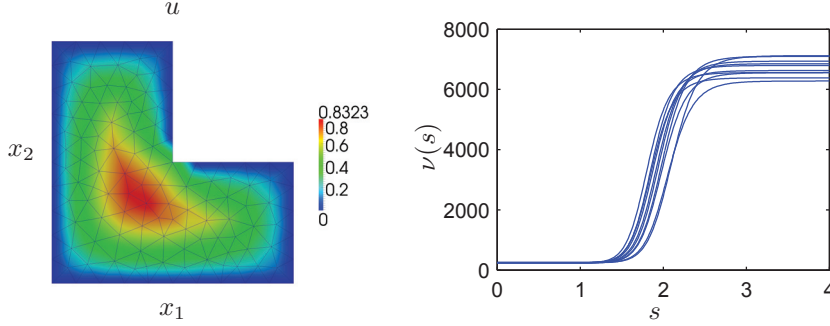


FIG. 6. *L-shaped domain. Left: solution evaluated with unperturbed material law and constant source current density $J = 10^5$ on the coarsest grid FE grid. Right: random realizations of stochastic material model (5.4).*

applied together with the constant excitation $J = 10^5$. We adopt the material model

$$(5.4) \quad \nu(s) = d + \frac{cs^{2b}}{a^b + s^{2b}}$$

from [21]. Given initial values $a_0 = 1.78$, $b_0 = 14$, $c_0 = 6000$ and $d_0 = 245$, we set $a = a_0(1 + 0.2Y_1)$, $b = b_0$, $c = c_0(1 + 0.2Y_2)$, and $d = d_0$ to introduce randomness, where $Y_{1,2} \sim \mathcal{U}(-\sqrt{3}, \sqrt{3})$. In Figure 6 on the left and right we depict the solution for $Y_1 = Y_2 = 0$ and random realizations of the reluctivity, respectively. Linearization is carried out as in the previous example. A coarse finite element (FE) grid as depicted in Figure 6 on the left, referred to as FE grid 1, is uniformly refined two (FE grid 2) and four times (FE grid 3), respectively. The stochastic error for a tensor grid $H_{q,2}^T$, w.r.t. both the polynomial degree and the number of grid points, is shown in Figure 7. As a reference, a higher order polynomial approximation ($q = 9$) in the stochastic variable is used on each grid. For this example there holds $\mathbf{grad} u \in \mathcal{H}^s(D)^2$, with $s = 2/3 - \epsilon$, with $\epsilon > 0$. According to Theorem 4.4 in 2D, see Remark 3, at least a decay of q^{-2} is expected as $s \in [1/2, 2/3)$. For the finest FE grid we numerically observe a decay of even $q^{-2.987}$. Hence, the convergence rate seems to be insensitive to the small ϵ parameter and the result could possibly be slightly improved. For grids 1 and 2 the decay is also faster than predicted. In Figure 8 the errors for a sparse $H_{q,2}^S$ are depicted. As $\lfloor i_s/M \rfloor = 1$ in this case, the convergence is assured. We observe an algebraic decay w.r.t. to the number of grid points. Also the tensor grid approach is more efficient in this case as, e.g., for $N_q = 49$ and FE grid 3, the error using $H_{q,2}^S$ is 4.12×10^{-4} , whereas the error using $H_{q,2}^T$ is 1.77×10^{-5} .

5.3. TEAM Benchmark. TEAM benchmarks are setup to validate electromagnetic codes and in particular magnetic field simulations. Here, we investigate the nonlinear magnetostatic TEAM 13 problem. A magnetic field in three thin iron sheets is generated by a rectangular coil, with blended corners, as depicted in Figure 9 on the right. Due to symmetry, only the upper half of the iron sheets is visualized. In a pre-processing step, an electrokinetic problem is solved to obtain the source current distribution \mathbf{J} with a total imposed current of 3000A per cross section. Gauging is enforced through a Lagrange multiplier and a mixed formulation see, e.g., [36]. The computational domain is truncated, applying homogeneous Dirichlet boundary conditions at a boundary, sufficiently far away from the problem setup. Strictly speaking

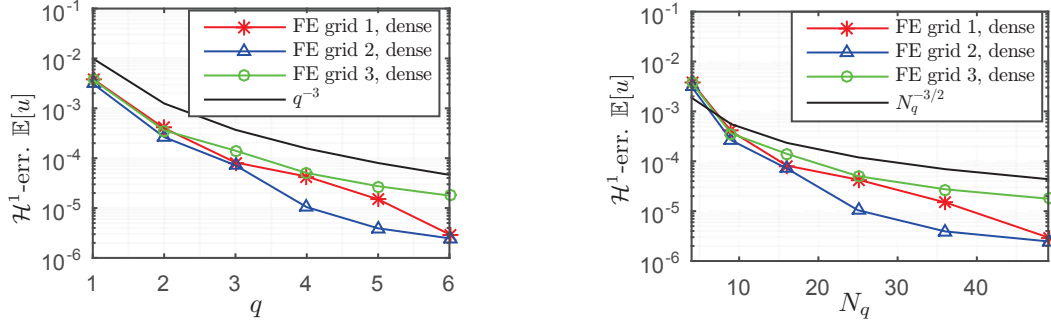


FIG. 7. L -shaped domain. Estimated stochastic error for tensor grid $H_{q,2}^T$ on three different FE grids. The reference solution is computed with polynomial degree $q = 9$. Left: error w.r.t. underlying polynomial degree. Right: error w.r.t. number of grid points.

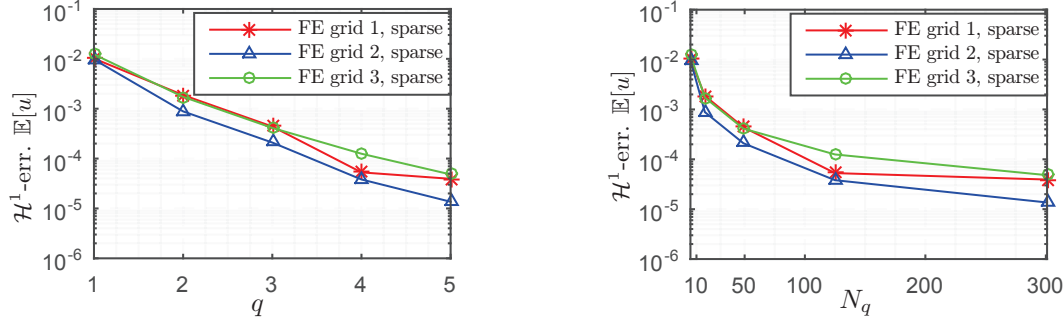


FIG. 8. L -shaped domain. Estimated stochastic error for sparse Smolyak grid $H_{q,2}^S$ on three different FE grids. The reference solution is computed on a dense grid with polynomial degree $q = 9$. Left: error w.r.t. sparse grid level. Right: error w.r.t. number of grid points.

this iron–air interface problem would require minor modifications of the analysis presented in this paper, as mentioned in Remark 1. We replaced the material properties of the original benchmark and employed the stochastic B – H curve presented in Section 3.2.1, with $L = 1/2$ and $\delta = 2$ instead. Extrapolation beyond the data range is carried out as described in [47]. Note that for this case we are concerned with \mathcal{C}^1 trajectories, solely. A tetrahedral mesh, see also Figure 9, is generated using the software Gmsh [28] and two steps of uniform refinement are carried out. We refer to the different FE grids with 7388, 41958 and 261196 total degrees of freedom as grid 1, 2 and 3, respectively. In Figure 9 on the left the magnetic flux density distribution is depicted for the expected value of the B – H curve. The nonlinear problem is linearized and iterated as explained in the p –Laplace example with a linearization increment below 10^{-5} in the discrete L^∞ –norm. In view of the expected low regularity of the solution and the small number of random inputs a tensor grid $H_{q,3}^T$ is used. The stochastic convergence is depicted in Figure 10 for all three FE grids. Here, the stochastic error is estimated as $\mathcal{H}(\text{curl})$ –norm of $\mathbb{E}[\mathbf{A}_{h,q,l}] - \mathbb{E}[\mathbf{A}_{h,q+1,l}]$, as we do not have an analytical solution. The initially rapid convergence deteriorates until the linearization error level is attained. We also observe that the convergence is algebraic. However, the convergence is faster than the predicted rate q^{-1} in view of the limited differentiability of the reluctivity.

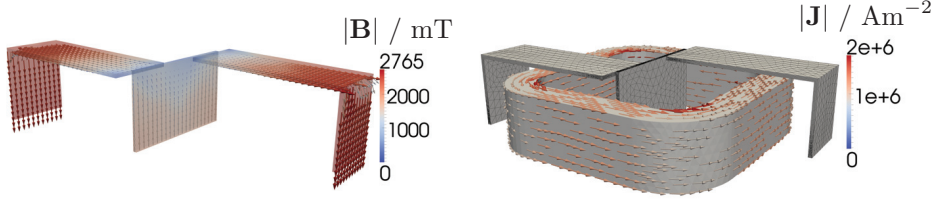


FIG. 9. *TEAM 13 problem. Left: magnetic flux density distribution in nonlinear material region for expected value of stochastic B - H curve. Right: source current distribution within coil and coarsest mesh of nonlinear material region.*

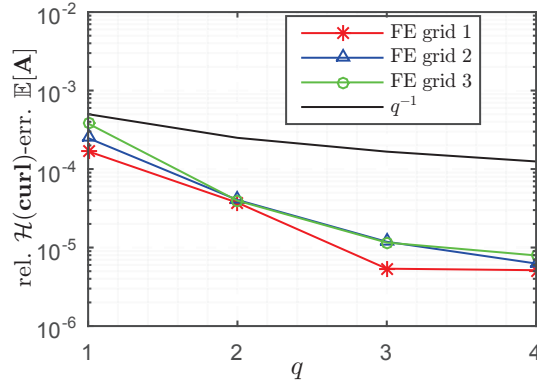


FIG. 10. *TEAM 13 problem. Estimated stochastic discretization error using $H_{q,3}^T$, i.e., $\mathcal{H}(\text{curl})$ -error of the expected value for different FE grids. Convergence is limited to the linearization error level.*

6. Conclusions. In this work, we have addressed the stochastic nonlinear elliptic curl-curl equation with uncertainties in the material law. Assumptions on the input have been formulated in order to obtain a well-posed stochastic formulation and it was shown that they can be fulfilled when a suitable discretization of the random input is carried out by the truncated Karhunen–Loève expansion. As monotonicity is required for the trajectories of the material law, oscillations can only occur with a rather small magnitude. A stability result for approximations of the random input was also derived. In the second part of the paper, a stochastic collocation method for the nonlinear curl-curl equation was analyzed. Under moderate differentiability assumptions on the material law, a convergence rate of q^{-k} was obtained for the stochastic collocation error using tensor grids, where $1 \leq k \leq 3$. For smooth boundaries and data this estimate holds true for all $k \in \mathbb{N}$. These estimates were shown to be in good agreement with numerical results for academic and benchmark examples. Convergence results for sparse grids were also obtained. However, in this case convergence can be expected only for a limited number of random input parameters.

Appendix A. Tensors. The tensors $D_{\mathbf{r}}^k \mathbf{h}$ for $1 \leq k \leq 3$, $\mathbf{s}_1, \mathbf{s}_2, \mathbf{s}_3 \in \mathbb{R}^3$ and $\mathbf{r} \neq 0$ read as

$$(A.1) \quad D_{\mathbf{r}}^1 \mathbf{h}(\cdot, \mathbf{r})(\mathbf{s}_1) = \frac{\nu^{(1)}(\cdot, |\mathbf{r}|)}{|\mathbf{r}|} \mathbf{r}(\mathbf{r} \cdot \mathbf{s}_1) + \nu(\cdot, |\mathbf{r}|) \mathbf{s}_1,$$

$$(A.2) \quad D_{\mathbf{r}}^2 \mathbf{h}(\cdot, \mathbf{r})(\mathbf{s}_1, \mathbf{s}_2) = \left(\frac{\nu^{(2)}(\cdot, |\mathbf{r}|)}{|\mathbf{r}|^2} - \frac{\nu^{(1)}(\cdot, |\mathbf{r}|)}{|\mathbf{r}|^3} \right) \mathbf{r}(\mathbf{r} \cdot \mathbf{s}_1)(\mathbf{r} \cdot \mathbf{s}_2) \\ + \frac{\nu^{(1)}(\cdot, |\mathbf{r}|)}{|\mathbf{r}|} ((\mathbf{r} \cdot \mathbf{s}_1)\mathbf{s}_2 + (\mathbf{r} \cdot \mathbf{s}_2)\mathbf{s}_1 + \mathbf{r}(\mathbf{s}_1 \cdot \mathbf{s}_2)),$$

and

$$(A.3) \quad D_{\mathbf{r}}^3 \mathbf{h}(\cdot, \mathbf{r})(\mathbf{s}_1, \mathbf{s}_2, \mathbf{s}_3) = \left(\frac{\nu^{(3)}(\cdot, |\mathbf{r}|)}{|\mathbf{r}|^3} - 3 \frac{\nu^{(2)}(\cdot, |\mathbf{r}|)}{|\mathbf{r}|^4} + 3 \frac{\nu^{(1)}(\cdot, |\mathbf{r}|)}{|\mathbf{r}|^5} \right) \mathbf{r}(\mathbf{r} \cdot \mathbf{s}_1)(\mathbf{r} \cdot \mathbf{s}_2)(\mathbf{r} \cdot \mathbf{s}_3) \\ + \left(\frac{\nu^{(2)}(\cdot, |\mathbf{r}|)}{|\mathbf{r}|^2} - \frac{\nu^{(1)}(\cdot, |\mathbf{r}|)}{|\mathbf{r}|^3} \right) (\mathbf{s}_3(\mathbf{r} \cdot \mathbf{s}_1)(\mathbf{r} \cdot \mathbf{s}_2) + \mathbf{r}(\mathbf{s}_3 \cdot \mathbf{s}_1)(\mathbf{r} \cdot \mathbf{s}_2) + \mathbf{r}(\mathbf{r} \cdot \mathbf{s}_1)(\mathbf{s}_3 \cdot \mathbf{s}_2)) \\ + \left(\frac{\nu^{(2)}(\cdot, |\mathbf{r}|)}{|\mathbf{r}|^2} - \frac{\nu^{(1)}(\cdot, |\mathbf{r}|)}{|\mathbf{r}|^3} \right) ((\mathbf{r} \cdot \mathbf{s}_1)\mathbf{s}_2 + (\mathbf{r} \cdot \mathbf{s}_2)\mathbf{s}_1 + \mathbf{r}(\mathbf{s}_1 \cdot \mathbf{s}_2))(\mathbf{r} \cdot \mathbf{s}_3) \\ + \frac{\nu^{(1)}(\cdot, |\mathbf{r}|)}{|\mathbf{r}|} ((\mathbf{s}_3 \cdot \mathbf{s}_1)\mathbf{s}_2 + (\mathbf{s}_3 \cdot \mathbf{s}_2)\mathbf{s}_1 + \mathbf{s}_3(\mathbf{s}_1 \cdot \mathbf{s}_2)),$$

respectively.

Appendix B. Sensitivity Analysis. Applying $\partial_{\mathbf{y}}^\gamma$, where $|\gamma|_1 = k$ to

$$(B.1) \quad \mathbf{curl}(\mathbf{h}(\mathbf{y}, \mathbf{curl} \mathbf{A}(\mathbf{y}))) = \mathbf{J},$$

we obtain

$$(B.2) \quad \mathbf{curl} \sum_{0 \leq \alpha \leq \gamma} \binom{\gamma}{\alpha} (\partial_{\mathbf{y}}^{\gamma-\alpha} \mathbf{h}_\alpha(\cdot, \mathbf{curl} \mathbf{A}(\mathbf{y}))) = 0.$$

Using Faà di Bruno's formula we expand

$$(B.3) \quad \partial_{\mathbf{y}}^\beta \mathbf{h}_\alpha(\cdot, \mathbf{curl} \mathbf{A}(\mathbf{y})) = \sum_{\pi \in \Pi(\beta)} D_{\mathbf{r}}^{\text{ca}(\pi)} \mathbf{h}_\alpha(\cdot, \mathbf{curl} \mathbf{A}(\mathbf{y})) (\mathbf{curl} \partial_{\mathbf{y}}^{\pi_1} \mathbf{A}(\mathbf{y}), \dots, \mathbf{curl} \partial_{\mathbf{y}}^{\pi_{\text{ca}(\pi)}} \mathbf{A}(\mathbf{y})),$$

where $\Pi(\beta)$ represents the set of partitions of β , $\text{ca}(\pi)$ the cardinality of $\pi = \{\pi_1, \dots, \pi_{\text{ca}(\pi)}\}$ and $\pi_i \subseteq \beta$ for $i = 1, \dots, \text{ca}(\pi)$, see [22, Theorem 2]. Then, equation (B.2) can be rewritten as

$$(B.4) \quad \mathbf{curl}(\nu_d(\cdot, \mathbf{curl} \mathbf{A}) \mathbf{curl} \mathbf{A}_\gamma) = -\mathbf{curl} \sum_{0 \leq \alpha \leq \gamma} \binom{\gamma}{\alpha} \left(\sum_{\pi \in \Pi^*(\gamma-\alpha)} D_{\mathbf{r}}^{\text{ca}(\pi)} \mathbf{h}_\alpha(\cdot, \mathbf{curl} \mathbf{A}) (\mathbf{curl} \mathbf{A}_{\pi_1}, \dots, \mathbf{curl} \mathbf{A}_{\pi_{\text{ca}(\pi)}}) \right),$$

where $\Pi^*(\gamma - \alpha)$ is defined as the set $\Pi(\gamma - \alpha)$, with $\text{ca}(\pi) > 1$ if $\alpha = 0$. We observe, that $\pi_i < \gamma$ for $i = 1, \dots, \text{ca}(\pi)$ and the summation carried out in the previous equation and hence the derivatives contained in the right-hand-side are of lower order.

Acknowledgment. The authors would like to thank Stéphane Clénet for providing measurement data of B – H curves and Herbert De Gersem for valuable comments and discussions on the subject.

REFERENCES

- [1] *Sparse grids matlab kit*. <http://csqi.epfl.ch>.
- [2] *Testing Electromagnetic Analysis Methods (T.E.A.M.)*. <http://www.compumag.org>.
- [3] C. AMROUCHE, C. BERNARDI, M. DAUGE, AND V. GIRAULT, *Vector potentials in three-dimensional non-smooth domains*, Mathematical Methods in the Applied Sciences, 21 (1998), pp. 823–864.
- [4] I. BABUŠKA AND P. CHATZIPANTELIDIS, *On solving elliptic stochastic partial differential equations*, Computer Methods in Applied Mechanics and Engineering, 191 (2002), pp. 4093–4122.
- [5] I. BABUŠKA, K.-M. LIU, AND R. TEMPONE, *Solving stochastic partial differential equations based on the experimental data*, Mathematical Models and Methods in Applied Sciences, 13 (2003), pp. 415–444.
- [6] I. BABUŠKA, F. NOBILE, AND R. TEMPONE, *A stochastic collocation method for elliptic partial differential equations with random input data*, SIAM Journal on Numerical Analysis, 45 (2007), pp. 1005–1034.
- [7] IVO BABUŠKA, FABIO NOBILE, AND RAÚL TEMPONE, *A stochastic collocation method for elliptic partial differential equations with random input data*, SIAM review, 52 (2010), pp. 317–355.
- [8] I. BABUŠKA, R. TEMPONE, AND G. ZOURARIS, *Solving elliptic boundary value problems with uncertain coefficients by the finite element method: the stochastic formulation*, Computer Methods in Applied Mechanics and Engineering, 194 (2005), pp. 1251–1294.
- [9] I. BABUŠKA, R. TEMPONE, AND G. E. ZOURARIS, *Galerkin finite element approximations of stochastic elliptic partial differential equations*, SIAM Journal on Numerical Analysis, 42 (2004), pp. 800–825.
- [10] F. BACHINGER, U. LANGER, AND J. SCHÖBERL, *Numerical analysis of nonlinear multiharmonic eddy current problems*, Numerische Mathematik, 100 (2005), pp. 593–616.
- [11] J. BÄCK, F. NOBILE, L. TAMELLINI, AND R. TEMPONE, *Stochastic spectral Galerkin and collocation methods for PDEs with random coefficients: a numerical comparison*, in Spectral and High Order Methods for Partial Differential Equations, J.S. Hesthaven and E.M. Ronquist, eds., vol. 76 of Lecture Notes in Computational Science and Engineering, Springer, 2011, pp. 43–62. Selected papers from the ICOSAHOM ’09 conference, June 22–26, Trondheim, Norway.
- [12] A. BARTEL, H. DE GERSEM, T. HÜLSMANN, U. RÖMER, S. SCHÖPS, AND T. WEILAND, *Quantification of uncertainty in the field quality of magnets originating from material measurements*, IEEE Transactions on Magnetics, 49 (2013), pp. 2367 – 2370.
- [13] VOLKER BARTHELMANN, ERICH NOVAK, AND KLAUS RITTER, *High dimensional polynomial interpolation on sparse grids*, Advances in Computational Mathematics, 12 (2000), pp. 273–288.
- [14] S. C. BRENNER AND R. SCOTT, *The mathematical theory of finite element methods*, Springer, 2008.
- [15] C. CANUTO AND T. KOZUBEK, *A fictitious domain approach to the numerical solution of pdes in stochastic domains*, Numerische mathematik, 107 (2007), pp. 257–293.
- [16] A. CHAILLOU AND M. SURI, *Computable error estimators for the approximation of nonlinear problems by linearized models*, Computer Methods in Applied Mechanics and Engineering, 196 (2006), pp. 210–224.
- [17] ———, *A posteriori estimation of the linearization error for strongly monotone nonlinear operators*, Journal of computational and applied mathematics, 205 (2007), pp. 72–87.
- [18] C. CHAUVIÈRE, J. S. HESTHAVEN, AND L. LURATI, *Computational modeling of uncertainty in time-domain electromagnetics*, SIAM Journal on Scientific Computing, 28 (2006), pp. 751–775.
- [19] ABDELLAH CHKIFA, ALBERT COHEN, AND CHRISTOPH SCHWAB, *Breaking the curse of dimensionality in sparse polynomial approximation of parametric pdes*, Journal de Mathématiques Pures et Appliquées, (2014).
- [20] ———, *High-dimensional adaptive sparse polynomial interpolation and applications to parametric pdes*, Foundations of Computational Mathematics, 14 (2014), pp. 601–633.
- [21] I. CIMRÁK, *Material and shape derivative method for quasi-linear elliptic systems with applications in inverse electromagnetic interface problems*, SIAM Journal on Numerical Analysis,

- 50 (2012), pp. 1086–1110.
- [22] D. E. CLARK AND J. HOUSSEINEAU, *Faa di bruno's formula for gateaux differentials and interacting stochastic population processes*, arXiv preprint arXiv:1202.0264, (2012).
 - [23] A. COHEN, R. DEVORE, AND C. SCHWAB, *Analytic regularity and polynomial approximation of parametric and stochastic elliptic pde's*, Analysis and Applications, 9 (2011), pp. 11–47.
 - [24] C. DE BOOR, *A practical guide to splines*, Springer-Verlag, New York.
 - [25] L. EL ALAOU, A. ERN, AND M. VOHRALÍK, *Guaranteed and robust a posteriori error estimates and balancing discretization and linearization errors for monotone nonlinear problems*, Computer Methods in Applied Mechanics and Engineering, 200 (2011), pp. 2782–2795.
 - [26] P. FRAUENFELDER, C. SCHWAB, AND R. A. TODOR, *Finite elements for elliptic problems with stochastic coefficients*, Computer Methods in Applied Mechanics and Engineering, 194 (2005), pp. 205–228.
 - [27] F. N. FRITSCH AND R. E. CARLSON, *Monotone piecewise cubic interpolation*, SIAM Journal on Numerical Analysis, 17 (1980), pp. 238–246.
 - [28] C. GEUZAIN AND J.-F. REMACLE, *Gmsh: A 3-d finite element mesh generator with built-in pre- and post-processing facilities*, International Journal for Numerical Methods in Engineering, 79 (2009), pp. 1309–1331.
 - [29] R. G. GHANEM AND P. D. SPANOS, *Stochastic finite elements: a spectral approach*, Springer, 1991.
 - [30] I. G. GRAHAM, S. JOE, AND L. H. SLOAN, *Iterated galerkin versus iterated collocation for integral equations of the second kind*, IMA Journal of Numerical Analysis, 5 (1985), pp. 355–369.
 - [31] B. HEISE, *Analysis of a fully discrete finite element method for a nonlinear magnetic field problem*, SIAM Journal on Numerical Analysis, 31 (1994), pp. 745–759.
 - [32] R. HIPTMAIR, *Finite elements in computational electromagnetism*, Acta Numerica, 11 (2002), pp. 237–339.
 - [33] A.G. JACK AND B.C. MECROW, *Methods for magnetically nonlinear problems involving significant hysteresis and eddy currents*, IEEE Transactions on Magnetics, 26 (1990), pp. 424–429.
 - [34] U. LANGER AND C. PECHSTEIN, *Coupled finite and boundary element tearing and interconnecting solvers for nonlinear potential problems*, ZAMM-Journal of Applied Mathematics and Mechanics/Zeitschrift für Angewandte Mathematik und Mechanik, 86 (2006), pp. 915–931.
 - [35] M. LOËVE, *Probability Theory*, vol. I-II, Springer New York, 1978.
 - [36] P. MONK, *Superconvergence of finite element approximations to Maxwell's equations*, Numerical Methods for Partial Differential Equations, 10 (1994), pp. 793–812.
 - [37] ———, *Finite element methods for Maxwell's equations*, Oxford University Press, 2003.
 - [38] M. MOTAMED, F. NOBILE, AND R. TEMPONE, *A stochastic collocation method for the second order wave equation with a discontinuous random speed*, Numerische Mathematik, 123 (2013), pp. 493–536.
 - [39] F. NOBILE AND R. TEMPONE, *Analysis and implementation issues for the numerical approximation of parabolic equations with random coefficients*, International Journal for Numerical Methods in Engineering, 80 (2009), pp. 979–1006.
 - [40] FABIO NOBILE, RAUL TEMPONE, AND CLAYTON G WEBSTER, *An anisotropic sparse grid stochastic collocation method for partial differential equations with random input data*, SIAM Journal on Numerical Analysis, 46 (2008), pp. 2411–2442.
 - [41] FABIO NOBILE, RAÚL TEMPONE, AND CLAYTON G WEBSTER, *A sparse grid stochastic collocation method for partial differential equations with random input data*, SIAM Journal on Numerical Analysis, 46 (2008), pp. 2309–2345.
 - [42] S. P. OLIVEIRA AND J. S. AZEVEDO, *Spectral element approximation of fredholm integral eigenvalue problems*, Journal of Computational and Applied Mathematics, 257 (2014), pp. 46–56.
 - [43] C PECHSTEIN, *Multigrid-newton-methods for nonlinear magnetostatic problems*, M.Sc. thesis, Johannes Kepler Universitt Linz, Austria, (2004).
 - [44] C. PECHSTEIN AND B. JÜTTLER, *Monotonicity-preserving interproximation of bh-curves*, Journal of Computational and Applied Mathematics, 196 (2006), pp. 45 – 57.
 - [45] R. RAMAROTAFIKA, A. BENABOU, AND S. CLÉNET, *Stochastic modeling of soft magnetic properties of electrical steels, application to stators of electrical machines*, IEEE Transactions on Magnetics, 48 (2012), pp. 2573–2584.
 - [46] M. M. RAO, *Probability Theory with Applications*, Academic Press, New York.
 - [47] S. REITZINGER, B. KALTENBACHER, AND M. KALTENBACHER, *A note on the approximation of b-h curves for nonlinear computations*, Tech. Report 02-30, SFB F013, Johannes Kepler University Linz, Austria, 2002.
 - [48] E. ROSSEEL, H. DE GERSEM, AND S. VANDEWALLE, *Nonlinear stochastic galerkin and collocation methods: Application to a ferromagnetic cylinder rotating at high speed*, Communications

- in Computational Physics, 8 (2010), pp. 947–975.
- [49] C. SCHWAB AND R. A. TODOR, *Karhunen–loève approximation of random fields by generalized fast multipole methods*, Journal of Computational Physics, 217 (2006), pp. 100–122.
 - [50] GERD WACHSMUTH, *Differentiability of implicit functions: Beyond the implicit function theorem*, Journal of Mathematical Analysis and Applications, 414 (2014), pp. 259–272.
 - [51] G. WELLS, K.-A. MARDAL, AND A. LOGG, *Automated solution of differential equations by the finite element method: The FEniCS book*, Springer, 2012.
 - [52] DONGBIN XIU AND JAN S HESTHAVEN, *High-order collocation methods for differential equations with random inputs*, SIAM Journal on Scientific Computing, 27 (2005), pp. 1118–1139.
 - [53] I. YOUSEPT, *Optimal control of quasilinear $H(\text{curl})$ -elliptic partial differential equations in magnetostatic field problems*, SIAM Journal on Control and Optimization, 51 (2013), pp. 3624–3651.
 - [54] E. ZEIDLER, *Nonlinear Functional Analysis and its Applications II/B, Nonlinear Monotone Operators, 1990*, Springer-Verlag, New York.